國立臺灣大學醫學院解剖學暨細胞生物學研究所

博士論文

Graduate Institute of Anatomy and Cell Biology

College of Medicine

National Taiwan University

Doctoral Dissertation

TMTC1 透過 integrins β1 和 β4 促進卵巢癌細胞侵襲

TMTC1 promotes invasiveness of ovarian cancer cells through integrins β1 and β4

葉庭芝 Ting-Chih Yeh

指導教授:黃敏銓博士 Min-Chuan Huang, Ph.D.

共同指導教授:陳啓豪博士 Chi-Hau Chen, Ph.D.

中華民國112年7月

July, 2023

doi:10.6342/NTU202302473

國立臺灣大學博士學位論文
口試委員會審定書

TMTC1 透過 integrins β1 和 β4 促進卵巢癌細胞侵襲
TMTC1 promotes invasiveness of ovarian cancer cells through integrins β1 and β4

本論文係葉庭芝君（學號 D05446009）在國立臺灣大學醫學院解剖學暨細胞生物學研究所完成之博士學位論文，於民國 112 年 06 月 02 日承下列考試委員審查通過及口試及格，特此證明

口試委員：黃敏銓
陳啓豪 （簽名）
（指導教授）
劉姮妤
王琳慧
龔秀妮

系主任、所長 陳玉怜 （簽名）

doi:10.6342/NTU202302473

誌謝

讀博士班時間，經歷過無數次的挑戰，終於盼到這一刻了，真的不容易。特別感謝黃敏銓老師，在我讀博士班的過程中仔細地教導我，對於研究方向與實驗方法提供適切的建議，讓我對於研究這條路，更加透徹了解。非常感謝陳啟豪醫師，在臨床上給予許多建議與幫助，讓我的博士論文能夠更加完整。也謝謝您積極地寫計畫，讓我有經費可以做實驗。謝謝林能裕老師，讓您的助理幫忙我做實驗還要一直聽壓力大的博士生啐啐念。感謝劉炯輝老師、王淑慧老師以及龔秀妮老師擔任我的口試委員，並提供許多建議。

在 revise 的過程中，非常感謝晉郁學弟特別停下自己的實驗，不分平日、假日盡力幫忙我補實驗，讓我能有充分時間寫回覆與 paper。也感謝子文學弟與軒羽學妹的幫忙，讓我能夠同步進行許多實驗。感激吳欣怡博士，幫忙解決質譜相關的問題與實驗。也要感謝實驗室的玫君學姊、瑩妤學姊、聖雯、又嘉、雅歆、儷元的陪伴。

最後我要感謝我的父母，有你們疼愛我的女兒子芸，我才能放心地完成學業。衷心感謝我的先生，從懷孕到小孩出生，一直扮演神隊友的角色，我才能順利度過難關。

doi:10.6342/NTU202302473

中文摘要

研究目的:卵巢癌是目前最致命的婦科惡性腫瘤。儘管O型甘露醣基轉移酶TMTC1在卵巢癌中有過度表現的情形，在卵巢癌中所扮演的角色仍然是未知的。

研究方法:透過免疫組織化學染色方法分析檢體中 TMTC1 的表現。經由卵巢癌細胞生長、移動、侵襲能力以及貼附的實驗，評估體外環境中的惡性特質。體內環境中的惡性特質則是藉由腹膜轉移測定。ConA 的 pull-down 以及醣蛋白質體技術則是用於鑑定 TMTC1 的受體。

研究結果:與鄰近的正常卵巢組織相比，TMTC1 在卵巢癌組織中有過度表現的狀況，且 TMTC1 過度表現與卵巢癌患者的不良預後明顯相關。降低 TMTC1 在卵巢癌細胞中的表現量，能夠抑制卵巢癌細胞的生長、移動、侵襲能力以及貼附。裸鼠的腹膜轉移測定中我們發現降低 TMTC1 的表現量，能夠抑制腹膜腫瘤的生長和轉移。另一方面，增加 TMTC1 在卵巢癌細胞中的表現量則是促進這些惡性特質。integrin β1 以及 β4 是 TMTC1 的受體，TMTC1 造成的移動與侵襲能力會被 integrin β1 或 β4 的 siRNA 阻斷。

研究結論: TMTC1 主要是透過調控 integrins β1 和 β4 的 O 型甘露醣基化而促進卵巢癌的細胞侵襲且是具有潛力的卵巢癌症治療分子標靶。

關鍵詞: TMTC1, O 型甘露醣基化, 卵巢癌， integrin β1, integrin β4

doi:10.6342/NTU202302473

Abstract

Objective. Among gynecological malignancies, the most lethal tumor is ovarian cancer. Although O-mannosyltransferase transmembrane and tetratricopeptide repeat containing 1 (TMTC1) exhibits high expression levels in ovarian cancer, no studies have investigated its precise role in ovarian cancer.

Methods. TMTC1 expression levels in clinical samples were examined by immunohistochemistry. Malignant properties of ovarian cancer cells were evaluated by MTT, transwell migration, Matrigel invasion, and adhesion assays *in vitro* and peritoneal xenograft assay *in vivo*. Protein substrates of TMTC1 were identified using Concanavalin A (ConA) pull-down assay and glycoproteomic analysis.

Results. In ovarian cancer patients, the expression of TMTC1 was found to be higher in the cancerous tissue specimens compared to the corresponding adjacent normal tissues. The high expression level of TMTC1 was significantly correlated with a poor prognosis among patients diagnosed with ovarian cancer. Knockdown of TMTC1 inhibited ovarian cancer cell viability, migration, invasion, and cell-laminin adhesion *in vitro*, in addition to inhibiting peritoneal tumor growth and metastasis *in vivo*. Conversely, TMTC1 overexpression promoted these malignant properties. Through mass spectrometry, integrins β1 and β4 were identified as new protein substrates of TMTC1. Notably, knockdown of integrin β1 or β4 was sufficient to reverse the TMTC1-induced migration

doi:10.6342/NTU202302473

and invasion.

Conclusions. TMTC1 facilitates the invasive behaviors of ovarian cancer cells mainly via integrins β1 and β4, making it a promising and potential target for therapeutic interventions in ovarian cancer.

Keywords: TMTC1, O-Man glycosylation, Ovarian cancer, integrin β1, integrin β4

doi:10.6342/NTU202302473

Contents

doi:10.6342/NTU202302473

doi:10.6342/NTU202302473

doi:10.6342/NTU202302473

doi:10.6342/NTU202302473

Figures

doi:10.6342/NTU202302473

doi:10.6342/NTU202302473

Tables

doi:10.6342/NTU202302473

Chapter I. Introduction

1.1 Ovarian cancer

Among gynecological malignancies, ovarian cancer is the most lethal tumor [1]. During a five-year study period (2003-2007), Europe, particularly Eastern and Southern Europe, had the highest occurrence of ovarian cancer. North and South America had intermediate incidence rates, while Oceania and Asia, including Hong Kong, Singapore, South Korea, Japan, and Thailand, had the lowest incidence rates. There were some variations in the incidence over time within specific regions. From the 1970s to the 2000s, ovarian cancer incidence decreased in North America and Northern Europe, but gradually increased in Eastern/Southern Europe and Asia, such as in Japan, South Korea, and Hong Kong [2]. According to statistical data from the United States, the mortality rate for ovarian cancer patients is as high as 64%. Regardless of ethnicity, whether they are White, Black, or from other racial backgrounds, approximately half of the patients diagnosed with ovarian cancer already have distant metastasis. The survival rate for such patients is only around 30%, resulting in an overall five-year survival rate for ovarian cancer patients of less than 50% [3]. The risk factors of morbidity include family genetic inheritance, use of hormone-related drugs after menopause in women aged 45 to 55, and infertility or women who have never given birth [4].

The available diagnostic tools for ovarian cancer, such as pelvic examination, vaginal

doi:10.6342/NTU202302473

ultrasound, and CA-125, suffer from limited sensitivity and precision, and so are not effective for early detection. Additionally, the ovary is in the deep pelvic cavity. There are no obvious symptoms at the beginning of ovarian cancer [5, 6]. Therefore, many patients are often diagnosed with late-stage ovarian cancer, with extensive metastasis of tumors within the peritoneal cavity. Acquiring a profound knowledge of the molecular mechanisms involved in the metastasis of ovarian cancer is crucial for enhancing patient outcomes. This knowledge will pave the way for the development of innovative therapeutic interventions.

Ovarian cancer can be classified into epithelial ovarian tumors, ovarian germ cell tumors, ovarian stromal tumors, and ovarian cysts based on histology. Among them, epithelial ovarian cancer is often diagnosed at an advanced stage and is the leading cause of gynecological cancer-related deaths. In addition to the general classification of epithelial ovarian cancer, it can be further subdivided into different histological subtypes, including high-grade serous ovarian cancer, low-grade serous ovarian carcinoma, mucinous carcinoma, endometrioid carcinoma, and clear-cell carcinoma. The pathological diagnosis of tumor tissue is crucial, as ovarian cancer encompasses various histological subtypes that require different treatment approaches. In the past decade, it has become evident that epithelial ovarian cancer is not a single disease but rather a collection of diseases with unique precursor lesions, tissue origins, molecular

doi:10.6342/NTU202302473

biology, clinical presentations, chemosensitivity, and patient outcomes [7].

1.2 Integrin

Integrins exert a strong influence on the interactions between epithelial cells and the extracellular matrix. The formation of a structural linkage by integrins between the interior and exterior of a cell enables the two-way transmission of signals, triggering a diverse array of cellular responses. This integration process assumes a pivotal role in the regulation of essential cellular processes, including cell adhesion, migration, proliferation, survival, and differentiation. By bridging the gap between the cell and its surrounding extracellular matrix, integrins serve as key mediators, orchestrating these crucial activities within the cell [8]. Integrins consist of α and β subunits that come together to form heterodimeric complexes. They belong to a large family of cell surface proteins. In mammals, researchers have identified 18 α subunits and 8 β subunits. The pairing of these subunits results in the formation of 24 distinct integrins. FAK serves as a key component within the signal transduction pathways triggered by integrins. Upon interaction between integrins and their specific ligands, FAK is recruited through their beta subunit. Autophosphorylation of FAK takes place, resulting in its interaction with Src and subsequent activation of both kinases. Subsequently, the active FAK/Src complex recruits p130CAS and paxillin, leading to the recruitment of Crk. This, in turn, activates Ras-related C3 botulinum toxin substrate 1 (RAC1), PAK, Jun aminoterminal

doi:10.6342/NTU202302473

kinase (JNK), and NFkB.

On the other hand, the FAK/Src complex can recruit and activate Ras-proximate-1 (RAP1), leading to the activation of ERK and MAPK through v-Raf murine sarcoma viral oncogene homolog B (BRAF). Moreover, the association of the FAK/Src complex with GRB2 can result in the activation of RAS, leading to the subsequent activation of the RAF-MEK-ERK pathway. Moreover, it has been observed that the interaction between PI3K and FAK leads to the stimulation of PI3K and the subsequent activation of its downstream signaling pathways. The integrin-FAK pathway plays a pivotal role in regulating a wide range of cellular functions, such as differentiation, growth, adhesion, migration, invasion, and survival, in both normal and tumor tissues [8-14]. Integrins play important roles in cancer metastasis. Hence, they present potential targets for cancer therapy.

Previous studies have also found the roles of integrins in ovarian cancer. The integrin α5 and its ligands are involved in the resistance to anoikis of ovarian cancer spheroids [15, 16]. Sawada et al. showed that downregulation of E-cadherin leads to upregulation in the expression of the fibronectin receptor α5β1-integrin. This upregulation facilitates the attachment of ovarian cancer cells to secondary metastasis sites, such as the peritoneum and omentum [17]. The overexpression of integrin β1 in ovarian cancer cells enhanced transwell migration and Matrigel invasion capabilities by modulating the PTEN/PI3K/Akt signaling

doi:10.6342/NTU202302473

pathway in response to fibrillar type I collagen matrices [18].

1.3 O-Man glycosylation

Protein glycosylation is a highly intricate post-translational modification, which regulates the function and structure of many membrane-bound and secreted proteins. O-Man glycosylation of proteins is a conserved form of glycosylation that is observed across various organisms, ranging from fungi to mammals [19]. During the process of O-Man glycosylation in the endoplasmic reticulum (abbreviated as ER), dolichol-phosphate mannose (abbreviated as Dol-P-Man) serves as the donor, transferring mannose to the serine (abbreviated as Ser) or threonine (abbreviated as Thr) residues of nascent polypeptides. A type of this reaction is modified by an active enzyme complex consisting of protein O-mannosyltransferase 1 (abbreviated as POMT1) and protein O-mannosyltransferase 2 (abbreviated as POMT2), where the primary substrate in mammals is α-dystroglycan (abbreviated as α-DG) [20, 21]. O-mannose glycans are vital for the development of muscle and brain tissues. Deficiency of these glycans on α-DG leads to congenital muscular dystrophies. POMT1 and POMT2 complex transfer O-mannose from the Dol-P-Man to an amino acid residue of serine or threonine via a covalent bond, forming an α-linkage bond. These proteins will assemble into either core M1 or core M2 before entering the Golgi apparatus. [20, 21].

doi:10.6342/NTU202302473

1.4 TMTC1

In 2017, a comprehensive range of O-mannosylated proteins was discovered, including cadherins/protocadherins, RON, c-MET receptor and plexins. Importantly, the O-Man glycosylation of these proteins does not involve the complex of POMT1 and POMT2 [22, 23]. TMTC1-4 have been recently identified as enzymes involved in the O-Man glycosylation of protocadherins and cadherins [22, 24]. TMTC1-mediated O-Man glycosylation differs from POMT1/POMT2-dependent O- mannosylation in that it does not undergo elongation into complex glycans. Instead, TMTC-mediated O-Man glycosylation is restricted to the addition of single O-Man monosaccharide structures [23]. The tetra-trico-peptide repeat (abbreviated as TPR) structure of TMTC1 is possessed by many proteins. It consists of thirty-four amino acids to form repeating sequences. TPR structure is composed of three to sixteen in tandem and regulates the interaction between proteins and generates multiprotein complexes. The TPR structure of TMTC1 is located near the endoplasmic reticulum (abbreviated as ER lumen) [25].

The correct localization of E-cadherin on the cell membrane is dependent on its O-Man glycosylation. The assembly of adherens junctions is affected by the alteration of O-Man glycosylation in gastric cancer cells [26]. The catalytic enzymes involved in O-Man glycosylation of plexins in mammalian cells are currently unidentified. A previous study showed that a high expression level of TMTC1 mRNA is related to poor survival

doi:10.6342/NTU202302473

of gastric cancer patients [27]. In prostate cancer, there is an overexpression of *TMTC4* mRNA compared to normal prostate tissues [28]. Despite the conservation of TMTC1-regulated O-Man glycosylation in mammalian cells and the expected relevance in cellular behaviors, the pathophysiological roles of TMTC1, TMTC2, TMTC3 and TMTC4 in many cancers are still undisclosed. Our study showed that higher TMTC1 expression was significantly related to poor prognosis in ovarian cancer patients. Both integrins β1 and β4 were identified as new protein substrates of TMTC1. Furthermore, TMTC1 enhanced the transwell migration and Matrigel invasion of ovarian cancer cells by modulating the O-Man glycosylation and activity of integrins β1 and β4. Notably, the inhibition of TMTC1 was found to effectively suppress ovarian cancer cells' invasiveness and peritoneal metastasis. Our data provide valuable insights into the mechanisms by which TMTC1 is involved in the pathogenesis of ovarian cancer.

Chapter II. Materials and methods

2.1 Cell lines and culture

Human ovarian cancer cell lines, including OVTW59 (The Department of Obstetrics and Gynecology at National Taiwan University gratefully acknowledges the generous contribution from Dr. P. L. Tong), were maintained in DMEM (Invitrogen), SKOV3 (ATCC) and ES-2 (ATCC) supplement with 10% FBS (Gibco) and 1% solution of

doi:10.6342/NTU202302473

penicillin/streptomycin (Gibco). All cells were maintained in a humidified atmosphere at 37°C with 95% air and 5% CO2.

2.2 Antibody generation and immunohistochemistry (IHC)

Biomax BC11115c and HOvaC154Su01 (tissue microarrays) were purchased for IHC. Ovarian cancer tissue microarrays were subjected to overnight incubation at 4°C with an in-house anti-TMTC1 antibody at a concentration of 2 μg/ml. The specific immunostaining was detected using the UltraVision™ Quanto Detection System HRP DAB (Thermo Fisher Scientific) with DAB Quanto Chromogen. Also, a counterstain of hematoxylin for one second was applied to all tissue microarrays.

The anti-TMTC1 antibody was produced through immunization of New Zealand White Rabbits with TMTC1 recombinant protein. The pGEX-4T-1 plasmid containing the TMTC1 insert was meticulously generated and subsequently transformed into highly competent BL21 E. coli cells. The induction of recombinant TMTC1 expression was initiated by adding 1 mM isopropyl-β-d-thiogalactoside (IPTG) when the A600nm value of the cultures reached 0.4 to 0.5, and the induction was carried out for 16 hours at 20°C. The inclusion body and soluble fractions were separated by utilizing a 9% SDS-PAGE gel and subsequently stained with Coomassie brilliant blue (Fig. 1A). The recombinant TMTC1 protein (65.8 kDa) on the 9% SDS-PAGE gel was transferred to a membrane. The membrane was incubated with New Zealand White Rabbit serum.

doi:10.6342/NTU202302473

Next, the anti-TMTC1 antibody bound to the PVDF membrane was eluted for subsequent use in IHC (Fig. 1B). Western blot analysis confirmed the detection of HA-tagged TMTC1 using the anti-TMTC1 antibody (Fig. 1C).

2.3 Real-time RT-PCR analysis

RNA extraction from ovarian cancer cells was performed using the TRIzol reagent (Invitrogen), followed by cDNA synthesis using the High Capacity cDNA Reverse Transcription Kit (Applied Biosystems). The cDNA was analyzed by real-time RT-PCR using specific primers targeting *GAPDH* (5'-TGAAGGTCGGAGTCAACGGATT-3' and 5'-CCTGGAAGATGGTGATGGGATT-3') or *TMTC1* (5'-TGTGTCAGAGGAGACCGGAT-3' and 5'-GGTTTCAGCTGGAGAGCCTT-3').

2.4 3-(4,5-dimethylthiazol-2-yl)-2,5-diphenyltetrazolium bromide assay (MTT)

The MTT assay, a widely used method for assessing cell viability, was employed to evaluate ovarian cancer cell viability. Briefly, 10 μl of MTT reagent (Sigma) at a concentration of 5 mg/ml was added to each well of a 96-well plate, followed by incubation at 37°C for three hours. Subsequently, the dissolving buffer, comprising 100 μl of a 0.01 N hydrochloric acid (HCl) solution supplemented with 10% sodium dodecyl sulfate (SDS), effectively dissolved the formazan crystals of MTT produced by the metabolically viable cells. Finally, an ELISA plate reader used to measure the absorbance at both 550 nm and 630 nm wavelengths.

doi:10.6342/NTU202302473

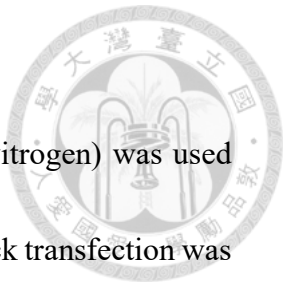

2.5 Transfection and plasmid construction

To investigate TMTC1 overexpression, Lipofectamine 3000 (Invitrogen) was used to transfect TMTC1/pRL-TK plasmids in ovarian cancer cells. A mock transfection was performed using the empty pRL-TK plasmid. On the other hand, ovarian cancer cells were transiently transfected with siRNA using Lipofectamine RNAiMAX (Invitrogen) for 48 hours to achieve *TMTC1* knockdown. We employed a negative control siRNA (5'-CAACCUCAGCCAUGUCGACUGGUUU-3') with medium GC content, along with two siRNA targeting TMTC1: siTMTC1-1 (5'-UGUCACCUUUGGGAGCACUGUAUUA-3') and si-TMTC1-3 (5'-ACGGUGUUUGGAGUGUGCUUGGUUU-3') obtained from Invitrogen. Besides, siRNAs against integrin β1 (si-ITGB1-1, 5'-CCUAAGUCAGCAGUAGGAACAUUAU-3' and si-ITGB1-2, 5'-UGCGAGUGUGGUGUCUGUAAGUGUA-3'), integrin β4 (si-ITGB4-1, 5'-GCCUACUGCACAGACGAGAUGUUCA-3' and si-ITGB4-2, 5'-CCGGAUGCUGCUUAUUGAGAACCUU-3') were also obtained from Invitrogen. As part of our research, we specifically procured the pLKO/TMTC1-shRNA plasmid (No. TRCN147171) and a comprehensive set of non-targeting pLKO plasmids (No. TRCN208001) from the National RNAi Core Facility at Academia Sinica, Taipei, Taiwan. Stable TMTC1 knockdown cells were successfully established with the shRNA

doi:10.6342/NTU202302473

construct in pLKO.1, utilizing a lentivirus-based transduction system. The ovarian cancer cells exhibiting stable *TMTC1* knockdown were specifically selected by treating them with 500 ng/ml puromycin for a duration of fourteen days. The confirmation of TMTC1 knockdown was systematically performed through comprehensive real-time RT-PCR analysis. Lentivirus-based transduction system was utilized to obtain overexpression of TMTC1 cells and corresponding control cells. This was achieved through transduction with negative control pLAS2w.Ppuro or pLAS2w.Ppuro-TMTC1-HA (RNAi Core; Academia Sinica). Subsequently, cells demonstrating stable knockdown of TMTC1 were selectively isolated by subjecting them to 14-day treatment with 500 ng/ml of puromycin.

2.6 Migration and invasion assay

We used 8-μm membrane chambers (Corning) for the transwell migration assay. The transwells were coated with Matrigel (BD Biosciences) for invasion assay. Ovarian cancer cells were gently detached using trypsin for 3 minutes and then suspended in a serum-free medium. They were then carefully seeded on the upper chamber. The chemoattractant used in the lower chamber was medium containing 10% FBS. After twenty-four hours of incubation, the ovarian cancer cells present on the lower surface of the chamber were subjected to crystal violet (Sigma) staining in a 20% (v/v) methanol solution and subsequently quantified under the microscope. These cells of

doi:10.6342/NTU202302473

each transwell were counted from four fields.

2.7 Adhesion assay

Laminin, fibronectin, collagen I, collagen IV, or the negative control Bovine Serum Albumin at a concentration of 5 μg/ml in Phosphate buffered saline were coated on six-well plates for three hours. Next, Six-well plates were blocked overnight with 1% Bovine Serum Albumin in sterilized Phosphate buffered saline at 4°C. Ovarian cancer cells ($4x10^5$) in 1 ml serum-free Dulbecco Modified Eagle Medium per well were carefully permitted to adhere to the pre-coated plates at 37°C for either 20 or 40 minutes. Subsequently, we used an inverted microscope to count the adhered cells.

2.8 LC-MS/MS analysis and database search

The extracellular domains of integrins β1 and β4, obtained from Sino Biological and used in our LC-MS/MS analysis were derived from HEK293 cells known for their high protein productivity. An LC-MS/MS analysis was performed on an Orbitrap Fusion Lumos Tribrid mass spectrometer with a quadrupole-ion trap (Thermo Fisher Scientific) and equipped with a nanospray interface, utilizing HCD and/or EThcD fragmentation techniques. To separate the peptides, the UltiMate 3000 nanoLC system (Thermo Fisher Scientific) was employed in conjunction with a mass spectrometer. In summary, peptides loaded with 2-μm particles featuring 100-A pores were introduced onto a 75-μm ID, 25-cm Acclaim PepMap C18 NanoLC column (Thermo Scientific). The LC-

doi:10.6342/NTU202302473

MS/MS analysis was conducted in a data-dependent mode with Full-MS, using a resolution of an automatic gain control (abbreviated as AGC) target of 5e5, 120,000 at m/z=200, and a maximum injection time of 50 msec. High-energy collision dissociation (HCD) MS/MS with a resolution of 15,000 was employed to fragment the most intense ions within a 1.4 Da isolation window at a normalized collision energy of 32% for a duration of 3 seconds. For MS/MS analysis, the AGC target was configured to 5e4, and previously selected ions were dynamically excluded for 180 seconds. The maximum injection time was set to 50 ms. The ETD reaction time for EThcD (resolution of 60,000) was configured to be 250 ms. The normalized collision energy was adjusted to 15% for HCD supplemental activation (calculated based on precursor m/z and charge state). For EThcD, the AGC target was set to 4e5.

Protein identification was conducted by utilizing the Mascot search algorithms (version 2.3) within the Proteome Discoverer package (version 2.2, Thermo Scientific) to search the raw MS/MS data against the Uniprot human database. The LC-MS/MS analysis data have been deposited to the ProteomeXchange Consortium through the PRIDE [18] partner repository, and the dataset has been assigned the identifier PXD037907.

2.9 ConA pull-down assay

To remove the N-glycans, we treated 250-1000μg of cell lysates with PNGase F

doi:10.6342/NTU202302473

(New England Biolabs). Following that, the lysates were subjected to overnight incubation at 4°C, utilizing ConA agarose beads (Vector Laboratories). Subsequently, we used PBS to wash the ConA agarose beads five times. The proteins that were pulled down were subsequently analyzed by Western blotting. To perform cell surface biotinylation, either TMTC1 siRNA (siTMTC1-1) or negative control siRNA (siControl) was transfected to OVTW59 cells. Following the biotinylation of surface molecules using Thermo Scientific EZ-Link Sulfo-NHS-Biotin, the ovarian cancer cell lysates underwent a 1-hour treatment with PNGase F. Subsequently, Concanavalin A-agarose beads were employed for the pull-down of glycoproteins containing mannose residues. The O-mannose changes were analyzed by detecting the biotinylated glycoproteins using streptavidin-horseradish peroxidase (abbreviated as HRP)-conjugated secondary antibodies and an enhanced chemiluminescence (abbreviated as ECL) kit.

2.10 Western blot analysis

NP40 buffer was used to extract cell pellets in order to obtain cell lysates. After being separated through electrophoresis on a 9% SDS-PAGE gel, the proteins were subsequently transferred onto a PVDF membrane. Following that, the PVDF membrane was blocked in 5% bovine serum albumin (Bio-Rad) at room temperature for 1 hour and incubated with a primary antibody against TMTC1 (in-house), p-FAK (Cell Signaling Technology), FAK (Santa Cruz Biotechnology), integrin β1 (BD

doi:10.6342/NTU202302473

Biosciences), integrin β4 (Cell Signaling Technology) or GAPDH (Santa Cruz Biotechnology) at 4°C overnight, respectively. Next, the PVDF membranes were subjected to incubation with secondary antibodies conjugated to HRP, followed by the detection of protein bands using ECL reagents (GE Healthcare Life Sciences).

2.11 Peritoneal metastasis assay

Nude mice (female) aged 5 to7 weeks were housed in sterilized cages with filtered air, sterilized bedding, and unrestricted access to special animal feed and treated water at the Animal Center of National Taiwan University College of Medicine. All animal studies were carried out following applicable regulations, guidelines, and protocols endorsed by the Animal Ethics Committee. First, 1 × 107 SKOV3 cells or 5 × 106 ES-2 cells were used for peritoneal injection of a nude mouse. At the respective time points of 40 or 15 days, the mice injected with SKOV-3 or ES-2 cells were sacrificed for further analysis. Subsequently, the extent of metastasis was evaluated by assessing the number and weight of formed metastatic nodules.

2.12 Statistical analysis

Statistical analysis of the tissue arrays was conducted with the SPSS 22.0 statistical software package. For other experiments, Kaplan-Meier plots, ANOVA, and Student's t-test were utilized. The results were shown as means ± SD, and statistical significance was determined by a two-sided P-value of less than 0.05.

doi:10.6342/NTU202302473

Chapter III. Results

3.1 Overexpression of TMTC1 in ovarian cancer

To investigate the expression profile of TMTC1 in different cancer tissues, we utilized RNA-seq data from seventeen cancer types obtained from the public database, The Cancer Genome Atlas (TCGA), for comparative analysis. The results showed that the expression levels of TMTC1 were found to be higher in ovarian tumors compared to other types of tumors (Fig. 2A).

3.2 Elevated TMTC1 expression level is correlated with poorer prognosis among patients diagnosed with ovarian cancer.

In order to assess the prognostic significance of TMTC1 expression in ovarian cancer patients, we extensively utilized the Kaplan-Meier plotter (abbreviated as KM plotter) public database, which contains microarray data. The results of Kaplan-Meier survival analysis revealed that patients with elevated TMTC1 expression exhibited significantly poorer survival in ovarian cancer (Fig. 2B). Subsequently, we evaluated the expression levels of TMTC1 in a tissue microarray (Biomax BC11115c) through immunohistochemical staining. The expression levels of TMTC1 were scored from 0 to 3 based on the intensity of the immunohistochemical staining (Fig. 2C). We found that, compared to normal tissues, cancerous ovarian specimens exhibited frequent overexpression of TMTC1 (Fig. 2D). Additionally, utilizing the clinical samples (n=116)

doi:10.6342/NTU202302473

derived from the tissue microarray (Biomax HOvaC154Su01), we categorized scores 0-1 as low TMTC1 expression and scores 2-3 as high TMTC1 expression. Furthermore, the Kaplan-Meier analysis consistently confirmed that elevated TMTC1 expression correlated with poor overall survival (Fig. 2E). Remarkably, the multivariate analysis revealed that, apart from the lymph node and distant metastasis, TMTC1 serves as an independent prognostic factor for poor prognosis (Table 1). These findings suggest that TMTC1 expression is upregulated in ovarian tumors and that high TMTC1 expression predicts poor survival among patients diagnosed with ovarian cancer.

3.3 TMTC1 expresses in ovarian cancer cells.

We investigated the endogenous levels of TMTC1 in ovarian cancer cells. Among the examined cell lines, SKOV3 cells displayed the highest expression level of **TMTC1**, whereas OVTW59 cells showed a subsequent higher expression level, and ES-2 cells exhibited the lowest expression level of *TMTC1* (Fig. 3). Consequently, For the *TMTC1* knockdown experiments, SKOV3 and OVTW59 cells were selected, while ES-2 cells were chosen for the TMTC1 overexpression experiments. Knockdown and overexpression of *TMTC1* were validated through real-time RT-PCR analysis (Fig. 4A). The average knockdown efficiencies of *TMTC1* in OVTW59 and SKOV3 cells were 82.7% and 78.4%, respectively. Conversely, the average overexpression efficiencies of TMTC1 in ES-2 cells were 1135.5 times higher compared to the control.

doi:10.6342/NTU202302473

3.4 TMTC1 promotes cell viability in ovarian cancer cells.

To explore the TMTC1 effects on malignant cell behaviors in vitro, we assessed cell viability in ovarian cancer cells through MTT assays. Our data from MTT assays showed that the knockdown of TMTC1 resulted in decreased cell viability, while the overexpression of TMTC1 led to increased cell viability (Fig. 4B).

3.5 TMTC1 promotes transwell migration and Matrigel invasion in ovarian cancer cells.

Afterwards, we evaluated the transwell migration and Matrigel invasion capabilities of ovarian cancer cells. The results obtained from the transwell migration assay showed a significant reduction in migration upon silencing of TMTC1 in SKOV3 and OVTW59 cells. Conversely, TMTC1 overexpression in ES-2 cells led to a notable increase in migration (Fig. 4C). In addition, the results obtained from the Matrigel invasion assay demonstrated a significant reduction in migration upon silencing of TMTC1 in SKOV3 and OVTW59 cells. On the other hand, TMTC1 overexpression in ES-2 cells resulted in a notable increase in migration (Fig. 4D). Furthermore, TMTC1 knockdown in ES-2 cells also resulted in decreased migration and invasion capabilities, consistent with the findings observed in SKOV3 and OVTW59 cells (Fig. 5). Taken together, these findings indicate that TMTC1 enhances the cell viability, transwell migration, and Matrigel invasion of ovarian cancer cells.

doi:10.6342/NTU202302473

3.6 TMTC1 enhances ovarian cancer cells' adhesion to laminin.

Based on the previous experiments, we found that migration and invasion are regulated by TMTC1. Additionally, the initial steps of potential metastasis were controlled by the interaction of adhesion receptors and proteases [29]. Therefore, our next step was to investigate whether TMTC1 affects cell adhesion. We investigated the impact of TMTC1 on cell adhesion to various extracellular matrix (abbreviated as ECM) proteins, such as collagen I, collagen IV, fibronectin, and laminin. Our findings of the adhesion assay revealed that silencing of TMTC1 in OVTW59 cells resulted in a significant reduction in cell adhesion to laminin (Fig. 6A). In addition, the silencing of TMTC1 in SKOV3 cells led to a reduction in cell-laminin adhesion (Fig. 6B). Conversely, the TMTC1 overexpression in ES-2 cells enhanced cell-laminin adhesion (Fig. 6B).

3.7 TMTC1 enhances FAK and AKT phosphorylation

Since cell-laminin adhesion is known to promote the FAK-AKT signaling pathway, we proceeded to analyze the phosphorylation of FAK at pY397 in ovarian cancer cells. ES-2, OVTW59 and SKOV3 cells were seeded on laminin-coated plates and subjected to Western blotting. As anticipated, the TMTC1 knockdown in OVTW59 and SKOV3 cells exhibited a decrease in FAK phosphorylation when these cells adhered to laminin (Fig. 6C). For more information, we quantified Western blots results of the

doi:10.6342/NTU202302473

phosphorylation of FAK and total FAK in these cells. The results indicated that the knockdown of TMTC1 led to a decrease in FAK phosphorylation (Fig. 7). By contrast, overexpression of TMTC1 resulted in increased pFAK in ES-2 cells. Moreover, a Western blot assay indicated that knockdown of TMTC1 decreased the phosphorylation of AKT, while TMTC1 overexpression significantly enhanced the phosphorylation of AKT (Fig 8). These findings showed that TMTC1 promotes cell-laminin adhesion and activates the downstream signaling pathway in ovarian cancer cells.

3.8 The integrins β1 and β4 O-Man glycosylation are modified by TMTC1 in ovarian cancer cells

In order to gain insights into the mechanism underlying the phenotypic changes induced by TMTC1 in ovarian cancer cells, we employed a glycoproteomic approach to identify the protein substrates of TMTC1. Due to ConA's affinity for glucose and mannose, TMTC1-regulated alterations in O-mannose can be identified using a ConA pull-down assay in the knockdown of TMTC1 or control ovarian cancer cells. N-glycans are rich in mannose, which could potentially affect the experimental results. Therefore, we pre-treated cell lysates with PNGase F. Our data showed that knockdown of TMTC1 in OVTW59 cells reduced the quantity of cell surface proteins pulled down by the ConA agarose beads (Fig. 9A), suggesting that ConA can identify TMTC1 protein substrates after the removal of N-glycans. Subsequently, we employed ConA

doi:10.6342/NTU202302473

agarose beads to capture the PNGase F-treated proteins in OVTW59 cells transfected with control or TMTC1 siRNA, followed by LC-MS/MS analysis. The findings revealed 17 proteins involved in the secretory pathway that exhibited decreased ConA binding (> 2-fold change) in the silencing of TMTC1 OVTW59 cells (Table 2). Cadherins/protocadherins have been identified as protein substrates of TMTC1-4. Our mass spectrometric results showed that the binding of ConA to protocadherin 7 exhibited a slight decrease of 0.87-fold in TMTC1 knockdown cells (Table 3). The O-Man glycosylation site in protocadherin 7 was confirmed to be S656 of peptide 650-ENLQPN''S''PVGMVTVMDADKGR-670 (Fig. 9B). In addition, the BioPlanet database showed that the functional pathway of the seventeen proteins is most closely related to integrin family cell surface interactions, followed by support of platelet aggregation by Eph kinases and ephrins (Table 4). The mass spectrometric data of SKOV3 cells also showed that ITGB1 is one of the top ten potential TMTC1 protein substrates (Table 5). Our data indicated that TMTC1 enhanced cell adhesion to laminin. Integrin β1 and integrin β4, identified as potential protein substrates of TMTC1, serve as receptors for laminin [4]. To investigate the existence of O-Man glycosylation on integrins β1 and β4, we analyzed integrins β1 and β4 from HEK293 cells using HCD and/or EThcTD mass spectrometry. The findings of HCD-MS/MS showed that seven O-mannosylated sites, S224, S263, S327, T333, S468, S474, and S587/S594, were

doi:10.6342/NTU202302473

identified in integrin β1 (Fig. 10). In addition, S387 was identified to be O-mannosylated on integrin β4 using EThcD-MS/MS analysis (Fig 11).

We then explored the role of integrins β1 and β4 in TMTC1-mediated effects. As expected, the results showed that the knockdown of TMTC1 resulted in reduced ConA binding to integrins β1 and β4 in OVTW59 and SKOV3 cells (Fig. 12A). We measured the levels of integrins β1 and β4 captured by ConA beads and evaluated the alterations in integrins β1 and β4 in OVTW59 cells with TMTC1 knockdown (Fig. 12B). The statistical analysis results demonstrated that knockdown of TMTC1 significantly reduced ConA binding to integrins β1 and β4 in OVTW59 cells, without altering the levels of integrins β1 and β4. On the contrary, the overexpression of TMTC1 enhanced the binding of integrins β1 and β4 to ConA in ES-2 cells. These results suggest that TMTC1 can modify the O-Man glycosylation of integrins β1 and β4 in ovarian cancer cells.

3.9 The involvement of EPHA2 in the TMTC1-regulated malignant phenotypes was found to be insignificant.

EPHA2 was identified as a potential TMTC1 protein substrate (Table 2). Nevertheless, analysis using a human phospho-RTK array revealed that the silencing of *TMTC1* did not result in significant changes in pRTK levels, including EPHA2 (Fig. 13).

doi:10.6342/NTU202302473

3.10 TMTC1 had no impact on the O-Man glycosylation of integrins α3 and α6.

Next, we investigated whether TMTC1 could modify the α subunits of integrins that bind to laminin. Specifically, we focused on four integrins, namely α3β1, α6β1, α7β1, and α6β4, which are known to interact with laminins as their extracellular ligands [30]. We examined the mRNA expression levels of integrins α3, α6 and α7 in ovarian cancer cells. The results showed that expression levels of integrins α3 and α6 were significantly increased compared to that of integrin α7 (Fig. 14A). Therefore, we selected integrin α3 and α6 for further ConA pull-down experiments, and the results showed that the silencing of *TMTC1* did not result in significant alterations in the expression levels of integrin α3 and α6 (Fig. 14B).

3.11 TMTC1 induced a slight enhancement in the heterodimerization between integrin α6 and β1.

To understand whether TMTC1-regulated O-Man glycosylation can regulate the association of integrin α and β subunits, we conducted co-immunoprecipitation (co-IP) assays in ES-2 and SKOV3 cells, respectively. In contrast, the overexpression of TMTC1 resulted in a slight increase in the heterodimerization between integrin α6 and β1, while the silencing of *TMTC1* led to a decrease in this heterodimerization (Fig. 15).

3.12 TMTC1 did not affect the mRNA expression of *MGAT5.*

An earlier investigation into target proteins of POMT2 revealed the presence of a

doi:10.6342/NTU202302473

synchronized interaction between the N-glycosylation and O-Man glycosylation pathways in gastric cancer. The mRNA expression transcript levels of *POMT2* and *MGAT5* showed a reciprocal relationship [26]. Based on data from real-time RT-PCR, the knockdown or overexpression of *TMTC1* did not result in significant changes in the transcript levels of *MGAT5* (Fig. 16).

3.13 *ITGB1* knockdown can reverse the TMTC1-induced effects on malignant phenotypes.

To examine the involvement of integrin β1 in the phenotypes regulated by TMTC1, we performed knockdown of ITGB1 in ovarian cancer cells stably transducted with knockdown or overexpression of TMTC1. We employed two separate siRNAs to knock down ITGB1 in stably transducted OVTW59 cells with knockdown of TMTC1, as well as ES-2 cells overexpressing TMTC1 (Fig. 17A and 17B). Transwell migration and Matrigel invasion analyses demonstrated that knockdown of integrin β1 reversed the migration and invasion suppression caused by TMTC1 shRNA in OVTW59 cells (Fig. 18A). When ITGB1 siRNAs were employed, the enhanced migration and invasion induced by TMTC1 were reversed in ES-2 cells (Fig. 18B). Based on our findings, it can be inferred that integrin β1 plays a pivotal role in the TMTC1-regulated ovarian cancer cells migration and invasion.

doi:10.6342/NTU202302473

3.14 *ITGB4* knockdown can reverse the TMTC1-induced effects on malignant phenotypes.

Subsequently, we explored the contribution of integrin β4 to the phenotypes modulated by TMTC1 by silencing integrin β4 in ovarian cancer cells with stable knockdown or overexpression of TMTC1. The OVTW59 cells stably transducted with TMTC1 were treated with two independent ITGB4 siRNAs (Fig. 17C). Similarly, the ES-2 cells stably transducted with TMTC1 were also treated with two independent ITGB4 siRNAs. (Fig. 17D). When ITGB4 siRNAs were utilized, the TMTC1 shRNA inhibitory effect on the transwell migration and Matrigel invasion of OVTW59 cells were reduced (Fig. 18C). Furthermore, the enhanced transwell migration and Matrigel invasion observed in ES-2 cells due to TMTC1 overexpression were reversed when ITGB4 siRNAs were used (Fig. 18D). Our findings suggest that integrin β4 also plays a vital role in the TMTC1-modulated ovarian cancer cells migration and invasion.

3.15 TMTC1 enhances the growth and metastasis of peritoneal tumors *in vivo*.

Ovarian cancer commonly develops peritoneal metastasis [19]. Hence, we evaluated TMTC1's impact on the growth and metastasis in the peritoneal cavity. Initially, we established stable ES-2 cells transfectants that exhibited overexpression of TMTC1 with an HA tag (Fig. 19A). Next, we injected stable ES-2 cells into nude mice intraperitoneally. The findings indicated that the overexpression of TMTC1 resulted in

doi:10.6342/NTU202302473

an elevation in tumor weights and an increase in the number of tumor nodules within the peritoneal cavity (Figs. 19B and 19C). Additionally, we generated stable transfectants of SKOV3 cells by transducting TMTC1 shRNA and subsequently injected these cells intraperitoneally into nude mice. Before conducting the animal experiments, we confirmed the gene silencing of TMTC1 using real-time RT-PCR analysis (Fig. 19D). TMTC1 knockdown resulted in a decrease in tumor weights and the number of tumor nodules within the peritoneal cavity (Figs. 19E and 19F). Based on these findings, it can be inferred that the growth and metastasis of ovarian cancer cells in the peritoneal region are facilitated by TMTC1. Although the results of survival analysis were not statistically significant, the mice injected with TMTC1-overexpressing ES-2 cells showed a similar trend of lower survival rate, as well as increased ascites, tumor numbers, and tumor weight compared to mice injected with control ES-2 cells (Fig. 20).

3.16 TMTC1 docking results and the therapeutic potential of targeting TMTC1 in human ovarian cancer treatment.

To search for the therapeutic potential of targeting TMTC1 in ovarian cancer treatment, we performed the I-TASSER method (http://zhanglab.ccmb.med.umich.edu/I-TASSER/) to model the protein structure of TMTC1 (Fig. 21). Then, we used ArnT as a template to perform docking simulation

doi:10.6342/NTU202302473

using the ZINC database (http://zinc.docking.org/). Similar to the POMT1/POMT2 enzymes, the TMTC1 protein exhibited a multi-pass transmembrane structure, featuring conserved DD motifs (predicted catalytic site) located in the first loop that faces the endoplasmic reticulum (ER) lumen. Furthermore, TMTC1 is predicted to possess structural similarity with both the POMTs and ArnT aminoarabinose-transferase. The top ten potential therapeutic protein substrates for targeting TMTC1 are listed (Table 6). These are the candidates for blocking TMTC1-mediated malignant phenotypes in ovarian cancer.

Chapter IV. Discussion

4.1 TMTC1 plays important roles in ovarian cancer

A considerable number of ovarian cancer patients are diagnosed at the third or fourth stage characterized by extensive dissemination within the peritoneal cavity [1, 31]. In order to enhance clinical outcomes, there is an immediate necessity to identify novel therapeutic targets that can aid in the development of agents aimed at inhibiting metastasis. In recent studies, TMTC1, TMTC2, TMTC3 and TMTC4 have been found to be new O-mannosyltransferases with mostly undisclosed protein substrates, apart from protocadherins and cadherins. TCGA database data have revealed that TMTC1 mRNA expression level is highest in ovarian cancer compared to sixteen other types of

doi:10.6342/NTU202302473

cancer. In this study, our research demonstrated that expression of the TMTC1 protein is markedly increased in ovarian cancer, and elevated TMTC1 levels are correlated with poor prognosis. In vitro studies demonstrate that TMTC1 enhances the growth and invasiveness of ovarian cancer cells, while in vivo experiments reveal its ability to enhance peritoneal growth and metastasis. In terms of mechanisms, TMTC1 plays a regulatory role in the O-Man glycosylation process and functionality of integrins β1 and β4, consequently facilitating transwell migration and Matrigel invasion (Fig. 22). Our data not only designate TMTC1 as a promising therapeutic target, but also enhance our comprehension of the involvement of TMTC1-regulated O-Man glycosylation in the development of ovarian cancer.

4.2 TMTC1 specifically modifies integrins β1 and β4 to promote the malignant behavior of ovarian cancer cells.

This study showed that TMTC1 modifies O-Man glycosylation of integrins β1 and β4, as well as downstream signaling molecules, including phosphorylation of FAK and AKT. Additionally, the transwell migration and Matrigel invasion ability of ovarian cancer cells, regulated by TMTC1, was reversed upon the application of siRNAs targeting integrin β1 or β4. Upregulation of integrins β1 and β4 is a common occurrence in ovarian cancer, playing a crucial role in promoting tumor progression, particularly metastasis in ovarian cancer [13, 32, 33]. Our findings revealed that TMTC1

doi:10.6342/NTU202302473

predominantly promotes cell adhesion to laminin with a comparatively minor effect observed on fibronectin. Additionally, TMTC1 exerts a slight influence on the heterodimerization of integrin α6 and β1. Different extracellular matrices (ECM) are cell adhesion receptors of different integrins. In the laminin-binding subfamily, the members include integrins α3β1, α6β1, α6β4, and α7β1 [34]. Prior evidence has indicated the significant involvement of integrins α6β1 and α6β4 in the progression of ovarian tumors [35, 36]. Integrin α5β1 also contributes to ovarian cancer cell invasion. Integrin β1 forms a crucial component of the primary fibronectin receptor, α5β1 [37]. The results provide compelling evidence that TMTC1 facilitates the invasiveness of ovarian cancer cells mainly via integrins β1 and β4.

4.3 O-Man glycosylation modulates the activities of integrins β1 and β4

A wide array of glycosylation modifications, encompassing O-linked and N-linked glycosylations, have been detected in numerous cancer cells. Activities of integrin are strongly regulated by glycans through glycan-mediated interactions and glycosylation events [38]. The presence of N-glycans on integrins can modulate their activities, thereby regulating migration processes and cell adhesion [38]. For instance, the N-glycosylation of Asn712 inhibits the responsiveness to EGF stimulation and EGFR dimerization, as well as influencing the formation of complexes between EGFR and integrin α5β1 or α6β4, which are involved in promoting cell growth [39]. Our research,

doi:10.6342/NTU202302473

along with other studies, has revealed that the functional activities of integrins are regulated by GalNAc-type O-glycosylation [11, 14, 40]. Our study represents the pioneering discovery of TMTC1-regulated O-Man glycosylation in integrins β1 and β4. Furthermore, this modification can augment the functionality of integrins β1 and β4, thereby facilitating cell adhesion to laminin. Remarkably, the α subunits prominently expressed in ovarian cancer cells are integrins α3 and α6, and our data revealed that TMTC1 had no significant impact on the O-Man glycosylation of these α subunits.

Our data indicate that TMTC1 exhibits a preference for substrates in integrins β1 and β4, suggesting that O-Man glycosylation occurs in these integrins. Our study is the first to offer mass spectrometry (MS)-based evidence confirming the presence of O-Man glycosylation sites on integrins β1 and β4. Further exploration into the role of TMTC1 in these specific sites and the functional significance of site-specific O-Man glycosylation in integrins β1 and β4 would be both intriguing and informative.

4.4 The regulation of ovarian cancer cell invasiveness by TMTC1 is unlikely to be mediated through its role in regulating calcium levels.

Besides being an O-mannosyltransferase, the TPR domains of the ER protein TMTC1 interact with SERCA2B, leading to a reduction in stimulated calcium release. This interaction is involved in maintaining ER calcium homeostasis [25]. TMTC1 overexpression inhibits the release of calcium from the ER upon stimulation proof by

doi:10.6342/NTU202302473

live cell calcium measurements. This observation suggests that reduced intracellular calcium levels may hinder the transwell migration and Matrigel invasion of ovarian cancer cells [41]. Nevertheless, our findings suggested that TMTC1 promotes the migration and invasion of ovarian cancer cells. Therefore, it is unlikely that the promotion of ovarian cancer transwell migration and Matrigel invasion by TMTC1 occurs through the regulation of calcium levels.

4.5 Targeting TMTC1 holds promise as a therapeutic strategy for ovarian cancer.

Our findings showed that expression levels of TMTC1 are upregulated in ovarian tumors and that higher TMTC1 expression predicts poor survival among patients diagnosed with ovarian cancer. Both in vitro and in vivo, TMTC1 enhances the invasiveness of ovarian cancer cells. Remarkably, the suppression of TMTC1 is sufficient to inhibit peritoneal tumor growth and dissemination. This study highlights both the important roles of TMTC1-regulated O-Man glycosylation in ovarian cancer biology and the potential of TMTC1 as a target for developing ovarian cancer theranostics in the future.

doi:10.6342/NTU202302473

References

1. Webb, P.M. and S.J. Jordan, *Epidemiology of epithelial ovarian cancer.* Best Pract Res Clin Obstet Gynaecol, 2017. **41**: p. 3-14.
2. Teng, Y.H., et al., *Epidemiology and Mortality of Ovarian Cancer in Taiwan: A Population-Based Study.* J Clin Med, 2022. **11**(19).
3. Siegel, R.L., et al., *Cancer statistics, 2022.* CA Cancer J Clin, 2022. **72**(1): p. 7-33.
4. Matulonis, U.A., et al., *Ovarian cancer.* Nat Rev Dis Primers, 2016. **2**: p. 16061.
5. Myers, E.R., et al., *Management of adnexal mass.* Evid Rep Technol Assess (Full Rep), 2006(130): p. 1-145.
6. Meany, D.L., L.J. Sokoll, and D.W. Chan, *Early Detection of Cancer: Immunoassays for Plasma Tumor Markers.* Expert Opin Med Diagn, 2009. **3**(6): p. 597-605.
7. Lheureux, S., et al., *Epithelial ovarian cancer.* Lancet, 2019. **393**(10177): p. 1240-1253.
8. Desgrosellier, J.S. and D.A. Cheresh, *Integrins in cancer: biological implications and therapeutic opportunities.* Nat Rev Cancer, 2010. **10**(1): p. 9-22.

doi:10.6342/NTU202302473

9. Hsu, W.M., et al., *B4GALNT3 expression predicts a favorable prognosis and suppresses cell migration and invasion via beta(1) integrin signaling in neuroblastoma.* Am J Pathol, 2011. **179**(3): p. 1394-404.

10. Chang, H.H., et al., *beta-1,4-Galactosyltransferase III enhances invasive phenotypes via beta1-integrin and predicts poor prognosis in neuroblastoma.* Clin Cancer Res, 2013. **19**(7): p. 1705-16.

11. Liu, C.H., et al., *C1GALT1 promotes invasive phenotypes of hepatocellular carcinoma cells by modulating integrin beta1 glycosylation and activity.* PLoS One, 2014. **9**(8): p. e94995.

12. Chen, C.H., et al., *beta-1,4-Galactosyltransferase III suppresses beta1 integrin-mediated invasive phenotypes and negatively correlates with metastasis in colorectal cancer.* Carcinogenesis, 2014. **35**(6): p. 1258-66.

13. Chen, C.H., et al., *MUC20 promotes aggressive phenotypes of epithelial ovarian cancer cells via activation of the integrin beta1 pathway.* Gynecol Oncol, 2016. **140**(1): p. 131-7.

14. Kuo, T.C., et al., *C1GALT1 high expression is associated with poor survival of patients with pancreatic ductal adenocarcinoma and promotes cell invasiveness through integrin alphav.* Oncogene, 2021. **40**(7): p. 1242-1254.

15. Carduner, L., et al., *Cell cycle arrest or survival signaling through alphav*

doi:10.6342/NTU202302473

integrins, activation of PKC and ERK1/2 lead to anoikis resistance of ovarian cancer spheroids. Exp Cell Res, 2014. **320**(2): p. 329-42.

16. Carduner, L., et al., *Ascites-induced shift along epithelial-mesenchymal spectrum in ovarian cancer cells: enhancement of their invasive behavior partly dependant on alphav integrins.* Clin Exp Metastasis, 2014. **31**(6): p. 675-88.

17. Sawada, K., et al., *Loss of E-cadherin promotes ovarian cancer metastasis via alpha 5-integrin, which is a therapeutic target.* Cancer Res, 2008. **68**(7): p. 2329-39.

18. Shen, Y., et al., *Fibrillar type I collagen matrices enhance metastasis/invasion of ovarian epithelial cancer via beta1 integrin and PTEN signals.* Int J Gynecol Cancer, 2012. **22**(8): p. 1316-24.

19. Neubert, P. and S. Strahl, *Protein O-mannosylation in the early secretory pathway.* Curr Opin Cell Biol, 2016. **41**: p. 100-8.

20. Vester-Christensen, M.B., et al., *Mining the O-mannose glycoproteome reveals cadherins as major O-mannosylated glycoproteins.* Proc Natl Acad Sci U S A, 2013. **110**(52): p. 21018-23.

21. Larsen, I.S.B., et al., *Multiple distinct O-Mannosylation pathways in eukaryotes.* Curr Opin Struct Biol, 2019. **56**: p. 171-178.

doi:10.6342/NTU202302473

22. Larsen, I.S.B., et al., *Discovery of an O-mannosylation pathway selectively serving cadherins and protocadherins.* Proc Natl Acad Sci U S A, 2017. **114**(42): p. 11163-11168.

23. Larsen, I.S.B., et al., *Mammalian O-mannosylation of cadherins and plexins is independent of protein O-mannosyltransferases 1 and 2.* J Biol Chem, 2017. **292**(27): p. 11586-11598.

24. Eisenhaber, B., et al., *Conserved sequence motifs in human TMTC1, TMTC2, TMTC3, and TMTC4, new O-mannosyltransferases from the GT-C/PMT clan, are rationalized as ligand binding sites.* Biol Direct, 2021. **16**(1): p. 4.

25. Sunryd, J.C., et al., *TMTC1 and TMTC2 are novel endoplasmic reticulum tetratricopeptide repeat-containing adapter proteins involved in calcium homeostasis.* J Biol Chem, 2014. **289**(23): p. 16085-99.

26. Carvalho, S., et al., *O-mannosylation and N-glycosylation: two coordinated mechanisms regulating the tumour suppressor functions of E-cadherin in cancer.* Oncotarget, 2016. **7**(40): p. 65231-65246.

27. Chen, X., Q. Zhang, and T. Chekouo, *Filtering High-Dimensional Methylation Marks With Extremely Small Sample Size: An Application to Gastric Cancer Data.* Front Genet, 2021. **12**: p. 705708.

28. Makboul, R., et al., *Transmembrane and Tetratricopeptide Repeat Containing*

doi:10.6342/NTU202302473

4 Is a Novel Diagnostic Marker for Prostate Cancer with High Specificity and Sensitivity. Cells, 2021. **10**(5).

29. Lengyel, E., *Ovarian cancer development and metastasis.* Am J Pathol, 2010. **177**(3): p. 1053-64.

30. Zent, R. and A. Pozzi, *Cell-extracellular matrix interactions in cancer*. 2010, New York: Springer. xii, 314 p.

31. Siegel, R.L., et al., *Cancer Statistics, 2021.* CA Cancer J Clin, 2021. **71**(1): p. 7-33.

32. Choi, Y.P., et al., *Targeting ILK and beta4 integrin abrogates the invasive potential of ovarian cancer.* Biochem Biophys Res Commun, 2012. **427**(3): p. 642-8.

33. Lee, J.G., et al., *Mutant p53 promotes ovarian cancer cell adhesion to mesothelial cells via integrin beta4 and Akt signals.* Sci Rep, 2015. **5**: p. 12642.

34. Arimori, T., et al., *Structural mechanism of laminin recognition by integrin.* Nat Commun, 2021. **12**(1): p. 4012.

35. Ahmed, N., et al., *Role of integrin receptors for fibronectin, collagen and laminin in the regulation of ovarian carcinoma functions in response to a matrix microenvironment.* Clin Exp Metastasis, 2005. **22**(5): p. 391-402.

doi:10.6342/NTU202302473

36. Stewart, R.L. and K.L. O'Connor, *Clinical significance of the integrin alpha6beta4 in human malignancies.* Lab Invest, 2015. **95**(9): p. 976-86.

37. Kenny, H.A., et al., *Mesothelial cells promote early ovarian cancer metastasis through fibronectin secretion.* J Clin Invest, 2014. **124**(10): p. 4614-28.

38. Marsico, G., et al., *Glycosylation and Integrin Regulation in Cancer.* Trends Cancer, 2018. **4**(8): p. 537-552.

39. Hang, Q., et al., *N-Glycosylation of integrin alpha5 acts as a switch for EGFR-mediated complex formation of integrin alpha5beta1 to alpha6beta4.* Sci Rep, 2016. **6**: p. 33507.

40. Zhang, C., et al., *Knockdown of C1GalT1 inhibits radioresistance of human esophageal cancer cells through modifying beta1-integrin glycosylation.* J Cancer, 2018. **9**(15): p. 2666-2677.

41. Liu, L., et al., *TRPM7 promotes the epithelial-mesenchymal transition in ovarian cancer through the calcium-related PI3K / AKT oncogenic signaling.* J Exp Clin Cancer Res, 2019. **38**(1): p. 106.

doi:10.6342/NTU202302473

Figures

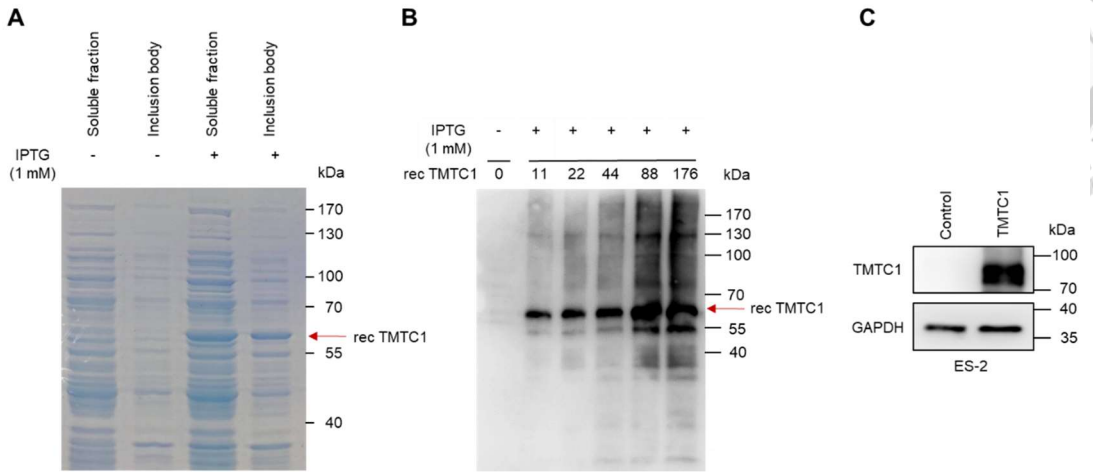

Figure 1. Generation of an anti-TMTC1 polyclonal antibody. (A) Recombinant TMTC1 protein expressed in BL21 competent E. coli was separated using a 9% SDS-PAGE gel. The BL21 competent E. coli cells were induced by 1 mM IPTG and cultured at a temperature of 20°C for a duration of 16 hours. The inclusion body (0.5 μg) and the soluble fraction (1.5 μg) protein of BL21 competent E. coli lysates were separated on a 9% SDS-PAGE gel and then stained with Coomassie brilliant blue. The recombinant TMTC1 protein (rec TMTC1) is indicated by the red arrow. (B) Western blot analysis showed the specific binding of the anti-TMTC1 antibody. Antibody against TMTC1 was generated in rabbits using recombinant TMTC1 as an antigen. The total proteins from the inclusion bodies were separated by a 9% SDS-PAGE, and the estimated concentrations of recombinant TMTC1 proteins were indicated. Subsequently, Western blotting was performed using the anti-TMTC1 antibody. The TMTC1 recombinant protein is indicated by the red arrow. (C) The anti-TMTC1 polyclonal antibody was utilized to detect the TMTC1 overexpression in ES-2 cells.

doi:10.6342/NTU202302473

The HA-tagged TMTC1, which was overexpressed in ES-2 cells, was captured using HA tag-agarose beads, followed by immunoblotting with the anti-TMTC1 antibody.

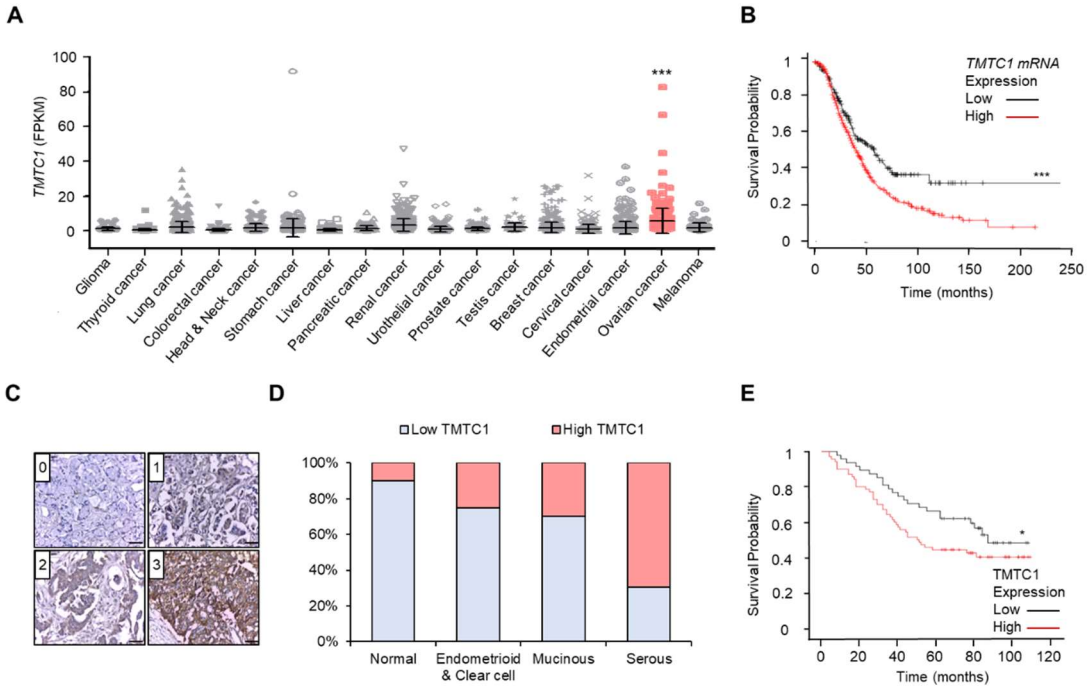

Figure 2. The expression level of TMTC1 is upregulated in ovarian cancer and elevated TMTC1 expression is correlated with poorer prognosis among patients diagnosed with ovarian cancer. (A) Expression levels of TMTC1 in different types of cancers were obtained from the TCGA database. In comparison to other cancer types, such as glioma (n=153), thyroid cancer (n=501), lung cancer (n=994), colorectal cancer (n=597), head and neck cancer (n=499), stomach cancer (n=354), liver cancer (n=365), pancreatic cancer (n=176), renal cancer (n=877), urothelial cancer (n=406), prostate cancer (n=494), testis cancer (n=134), breast cancer (n=1075), cervical cancer (n=291), endometrial cancer (n=541), and melanoma (n=102), the mRNA levels of TMTC1 were

doi:10.6342/NTU202302473

significantly elevated in the tumor tissues of 373 serous ovarian cancer patients. Expression quantification was performed using the fragments per kilobase of exon per million mapped fragments (FPKM) for TMTC1 with a detection threshold set at 1 FPKM. Data were analyzed using one-way ANOVA. ***P < 0.001. (B) Overall survival analysis was conducted using the Kaplan-Meier plotter, considering the expression ranges of the probes spanning from 3 to 4993. The Kaplan-Meier plotter utilized a probe value of 201 as the cut-off point to categorize TMTC1 expression into high and low groups. The cohort with low expression demonstrated a median survival period of 57.1 months, while the cohort with high expression experienced a median survival period of 40 months. The analysis conducted by the Kaplan-Meier plotter included all histological subtypes and grades. There were 444 patients with high (red) TMTC1 expression and 211 patients with low (black) TMTC1 expression. ***P < 0.001. (C) The TMTC1 levels in ovarian cancer tissues were assessed and assigned scores ranging from 0 to 3 based on immunostaining with an anti-TMTC1 antibody. The scale bar represents 0.5 mm. (D) Immunohistochemical analysis was conducted to evaluate the levels of TMTC1 in ovarian tumors (n = 90), comprising 62 serous carcinomas, 10 mucinous carcinomas, 5 clear cell carcinomas, and 3 endometrioid carcinomas, as well as adjacent normal ovary tissues (n = 10). (E) The Kaplan-Meier survival curve was generated for overall survival in ovarian cancer. TMTC1 expression in tissue

doi:10.6342/NTU202302473

microarrays was categorized into two groups: low (0-1; n = 43) and high (2-3; n = 73). Specimens from metastatic sites, cases with missing data, and rare histologic types were excluded from the analysis. The final dataset included 2 clear cell types, 13 endometrioid, 30 mucinous, 57 high-grade serous and 14 low-grade serous. *P < 0.05; ***P < 0.001.

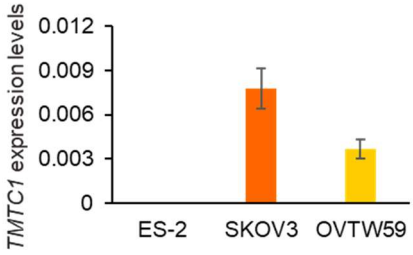

Figure 3. The endogenous TMTC1 expression levels were detected in ovarian cancer cells. *TMTC1* mRNA levels were analyzed in OVTW59 (0.00369159), SKOV3 (0.00775734), and ES-2 (0.00000785) cells through real-time RT-PCR. The TMTC1 mRNA levels were examined using real-time RT-PCR and then normalized to the mRNA levels of GAPDH, resulting in the formation of relative transcript levels. These data are reported as the mean ± standard deviation (SD).

doi:10.6342/NTU202302473

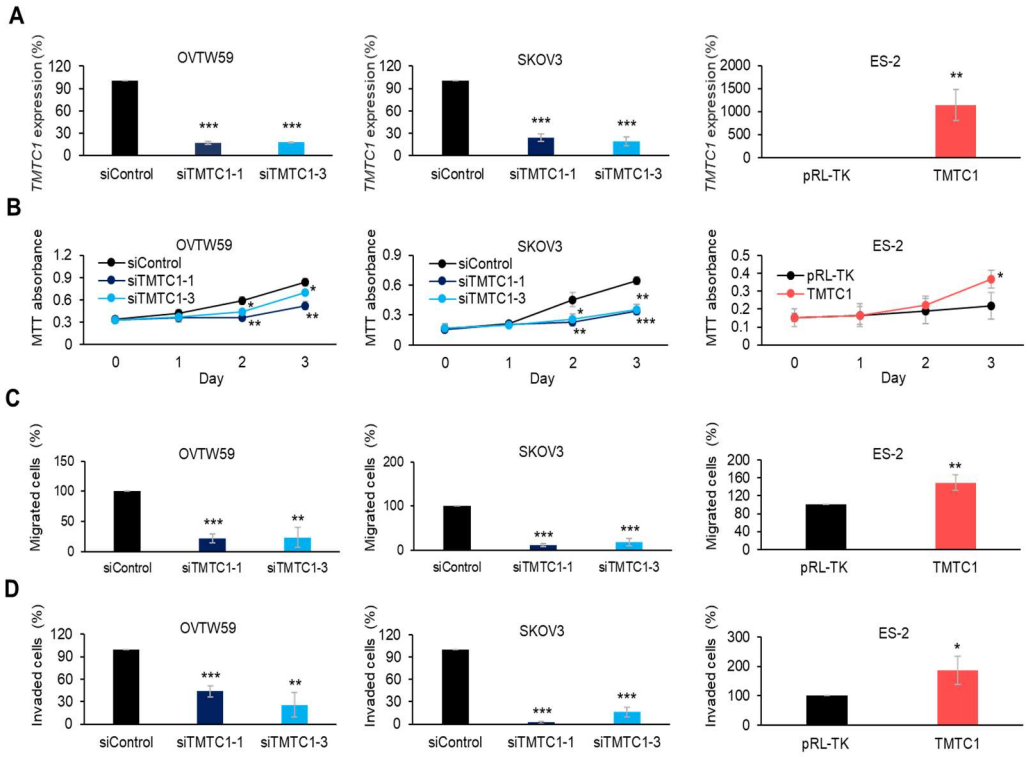

Figure 4. TMTC1 enhances malignant phenotypes in ovarian cancer cells. TMTC1 promotes malignant phenotypes in ovarian cancer cells. (A) OVTW59 and SKOV3 cells were transfected with either a non-targeting siRNA (siControl) or two independent siRNAs specifically targeting TMTC1 (siTMTC1-1 and siTMTC1-3). The transfections were carried out for a period of 48 hours. ES-2 cells were transfected with either pRL-TK/TMTC1 or empty pRL-TK plasmid for 48 hours. The TMTC1 transcript levels were examined using real-time RT-PCR and normalized to the mRNA levels of GAPDH, resulting in the formation of relative transcript levels. (B) TMTC1 effects on cell viability. Cells (OVTW59 and SKOV3 cells) with higher expression of TMTC1 were treated with siTMTC1-1 and siTMTC1-3, while siControl was used as the control.

doi:10.6342/NTU202302473

Cells with lower expression of TMTC1 (ES-2 cells) were subjected to overexpression of TMTC1 using the pRL-TK/TMTC1 (TMTC1) plasmid, while an empty pRL-TK plasmid was used as the control. Initially, 1 × 103 ovarian cancer cells were seeded into 96-well plates. Viable cells were assessed using the MTT assay at various time points, as indicated. (C) TMTC1 effects on migration. Following a 48-hour transfection, 3.5 × 104 OVTW59, 1 × 104 SKOV3, and 1 × 104 ES-2 cells were seeded for the transwell migration assay. The lower chamber of the transwell system contained 10% FBS, serving as a chemoattractant. After incubation for 24 hours, migrated cells were counted from four fields under an inverted microscope. (D) TMTC1 effects on invasion. Following a 48-hour transfection, 3.5 × 104 OVTW59, 1 × 104 SKOV3, and 1 × 104 ES-2 cells were seeded for the Matrigel invasion assay. After a 24-hour incubation period, the count of invaded cells was recorded. The obtained data were evaluated utilizing the Student's t-test. The results are reported as the mean ± SD (n = 3). *P < 0.05; **P < 0.01; ***P < 0.001.

doi:10.6342/NTU202302473

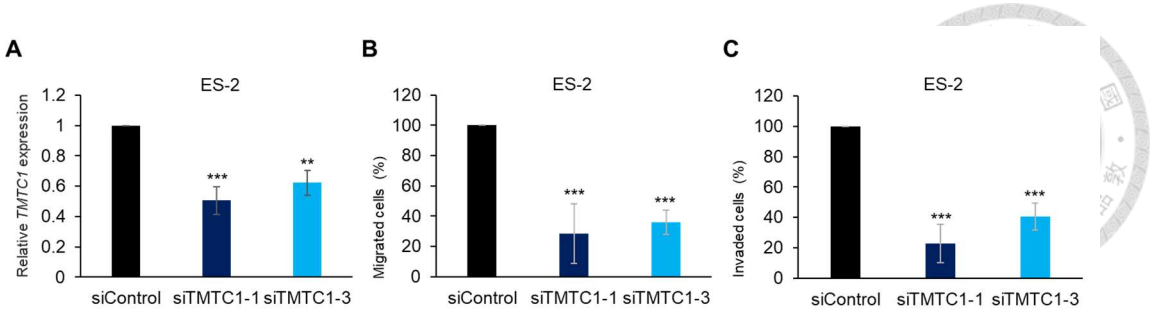

Figure 5. Knockdown of TMTC1 inhibits malignant phenotypes in ES-2 cells. (A) To achieve TMTC1 knockdown in ES-2 cells, transfections were performed using siControl as the control group and siTMTC1-1 and siTMTC1-3 as the experimental groups, with a duration of 48 hours. Real-time RT-PCR was employed to quantify the relative levels of TMTC1 transcripts, normalized to the mRNA levels of GAPDH. (B) The influence of TMTC1 on cell migration. After 48-hour transfection, ES-2 cells were seeded at a density of 1 × 104 cells for the transwell migration assay. The lower chamber of the transwell system contained 10% FBS, serving as a chemoattractant. After incubation for 24 hours, migrated cells were counted from four fields under an inverted microscope. (C) TMTC1 effects on cell invasion. Following a 48-hour transfection, 1 × 104 ES-2 cells were seeded for the Matrigel invasion assay. After incubation for 24 h, migrated cells were counted from four fields under an inverted microscope. The data are expressed as the mean ± SD. **P < 0.01; ***P < 0.001

doi:10.6342/NTU202302473

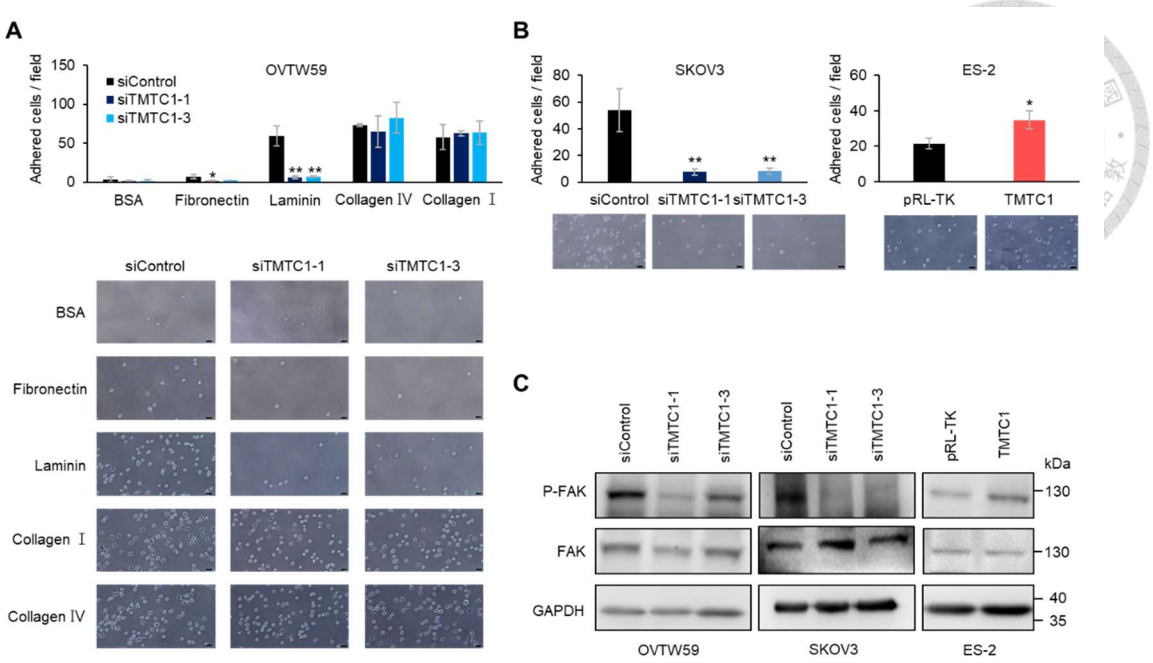

Figure 6. TMTC1 enhances the adhesion of ovarian cancer cells to laminin. (A) Cell-ECM adhesion assay. *TMTC1* knockdown OVTW59 cells were seeded into 96-well plates coated with 5 μg/mL fibronectin, laminin, collagen I or collagen IV; BSA was used as a control. Following a 20-minute incubation at 37°C, adhered cells were counted in four microscopic fields. Representative images were shown in the lower panel. Representative results from three independent experiments were shown. Data were analyzed using the Student's *t*-test. **P* < 0.05; ***P* < 0.01. (B) Cell-laminin adhesion assay. SKOV3 cells with *TMTC1* knockdown and ES-2 cells with *TMTC1* overexpression were seeded onto 5 μg/mL laminin-coated 96-well plates. The number of adhered cells was quantified in four microscopic fields. Representative images were shown in the lower panel. Representative results from three independent experiments are presented. Results are presented as mean ± SD (*n* = 3). Data were analyzed using

doi:10.6342/NTU202302473

the Student's *t*-test. *$P < 0.05$; **$P < 0.01$. (C) The effect of TMTC1 on laminin-mediated tyrosine phosphorylation of FAK was assessed. OVTW59 and SKOV3 cells with *TMTC1* knockdown and ES-2 cells with TMTC1 overexpression were seeded onto culture plates coated with 5 μg/mL of laminin in serum-free DMEM. Changes in FAK phosphorylation (pY397) were assessed using Western blotting, with GAPDH serving as the internal control.

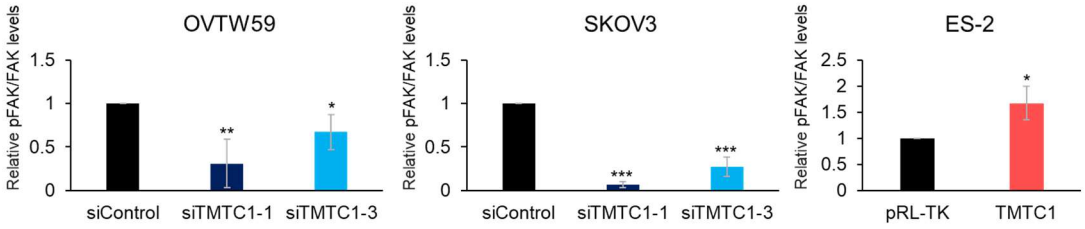

Figure 7. Quantification of phosphorylated FAK and total FAK in ovarian cancer cells. The Visionworks software was utilized to quantify the relative signal intensities of Phospho-FAK and total FAK on Western blots in Figure 6C. The resulting ratio of Phospho-FAK /FAK was shown. **$P < 0.01$; **$P < 0.01$; ***$P < 0.001$.

doi:10.6342/NTU202302473

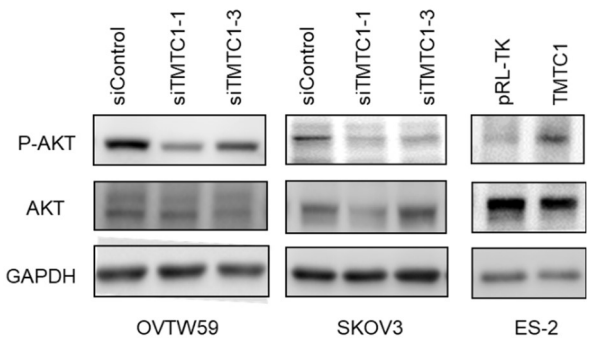

Figure 8. The effects of TMTC1 knockdown on AKT tyrosine phosphorylation. TMTC1 effects on laminin-regulated tyrosine phosphorylation of AKT. Human ovarian cancer cells were plated on 6-well plates coated with a concentration of 5 μg/mL laminin in serum-free DMEM and incubated for 20 minutes. Signal intensity changes in pAKT were assessed using Western blotting, with GAPDH serving as the internal control.

doi:10.6342/NTU202302473

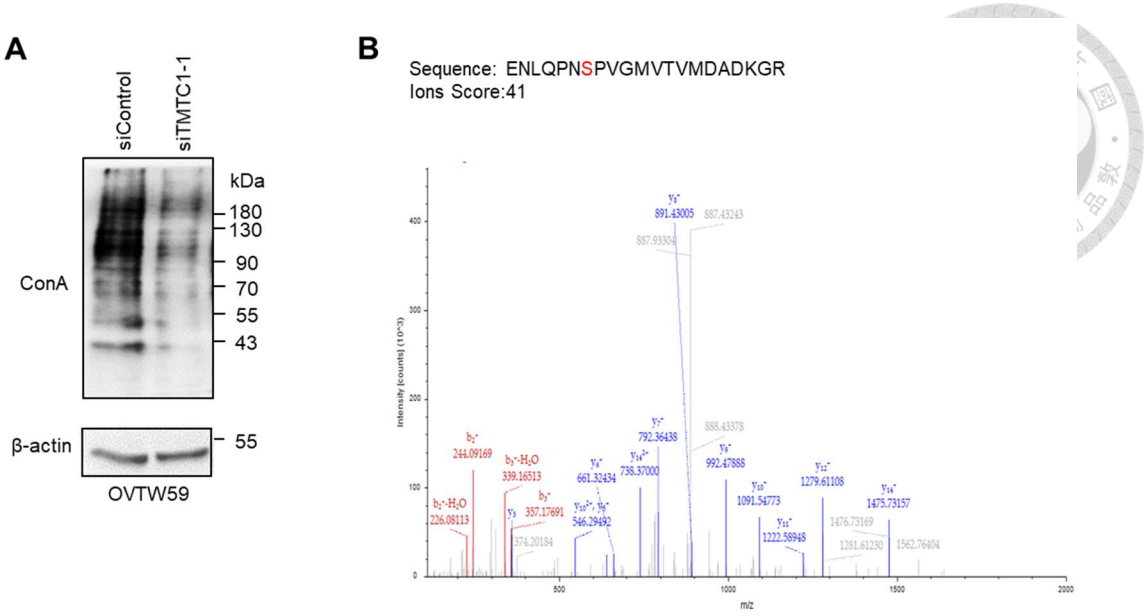

Figure 9. TMTC1 modifies the O-Man glycosylation of ovarian cancer cells. (A) Cell surface biotinylation and ConA pull-down assay for TMTC1. Control siRNA or siTMTC1-1 were transfected into OVTW59 cells. Total cell lysates were subjected to treatment with PNGase F to enzymatically remove N-glycans after cell surface labeling with biotin. Next, Glycoproteins with mannoses were captured using ConA-agarose beads. The detection of biotinylated glycoproteins was performed using streptavidin-HRP and an ECL kit. (B) The O-Man glycosylation site on protocadherin 7 was identified in OVTW59 cells. We mapped the O-Man glycosylation site on 650-ENLQPN"S"PVGMVTVMDADKGR-670 of protocadherin 7 using HCD fragmentation during MS/MS analysis. The presence of ion y14+ indicated that S656 was potentially O-mannosylated. The peptide's ion score for this observation was 41.

doi:10.6342/NTU202302473

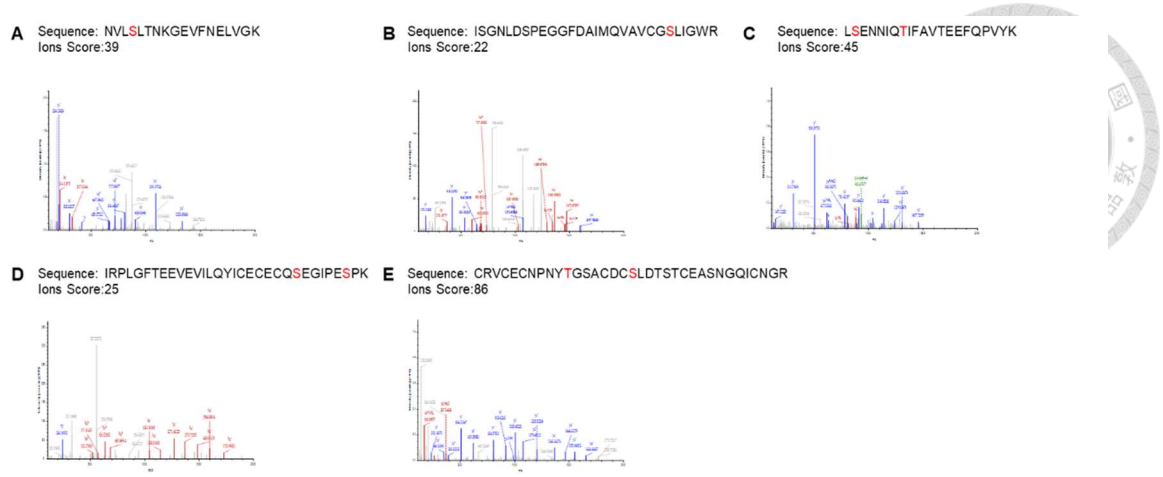

Figure 10. O-Man glycosylation sites present on integrin β1. The integrin β1 protein derived from HEK293 cells underwent analysis using HCD-MS/MS. (A) The presence of ions $b3^{+}$ and $y14^{2+}$ indicated that S224 on the peptide NVLSLTNKGEVFNELVGK was potentially O-mannosylated. (B) The presence of ions $b15^{+}$ and $y5^{+}$ indicated that S263 on the peptide ISGNLDSPEGGFDAIMQVAVCGSLIGWR was potentially O-mannosylated. (C) The presence of ions $y12^{+}$ indicated that S327 and T333 on the peptide LSENNIQTIFAVTEEFQPVYK were potentially O-mannosylated. (D) The presence of ions $b15^{+}$ and $y2^{+}$ indicated that S468 and S474 on the peptide IRPLGFTEEVEVILQYICECECQSEGIPESPK were potentially O-mannosylated. (E) The presence of ions $b42^{+}$ and $y15^{+}$ indicates that S587 or S594 on the peptide CRVCECNPNYTGSACDCSLDTSTCEASNGQICNGR were potentially O-mannosylated. The red-colored amino acids indicated the presence of O-Man glycosylation.

doi:10.6342/NTU202302473

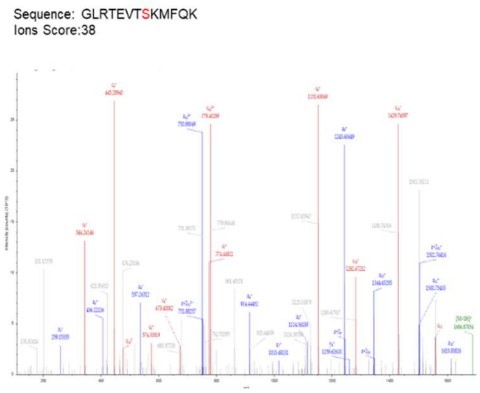

Figure 11. O-Man glycosylation sites present on integrin β4. The O-Man glycosylation site on the sequence 380-GLRTEVTSKMFQK-392 of integrin β4 derived from HEK293 cells was determined using EThcD fragmentation during MS/MS analysis. The presence of ions $c7^+$, $c9^+$, $z4^+$, and $z6^+$ indicates that S387 was potentially O-mannosylated. The peptide's ion score for this observation was 38.

doi:10.6342/NTU202302473

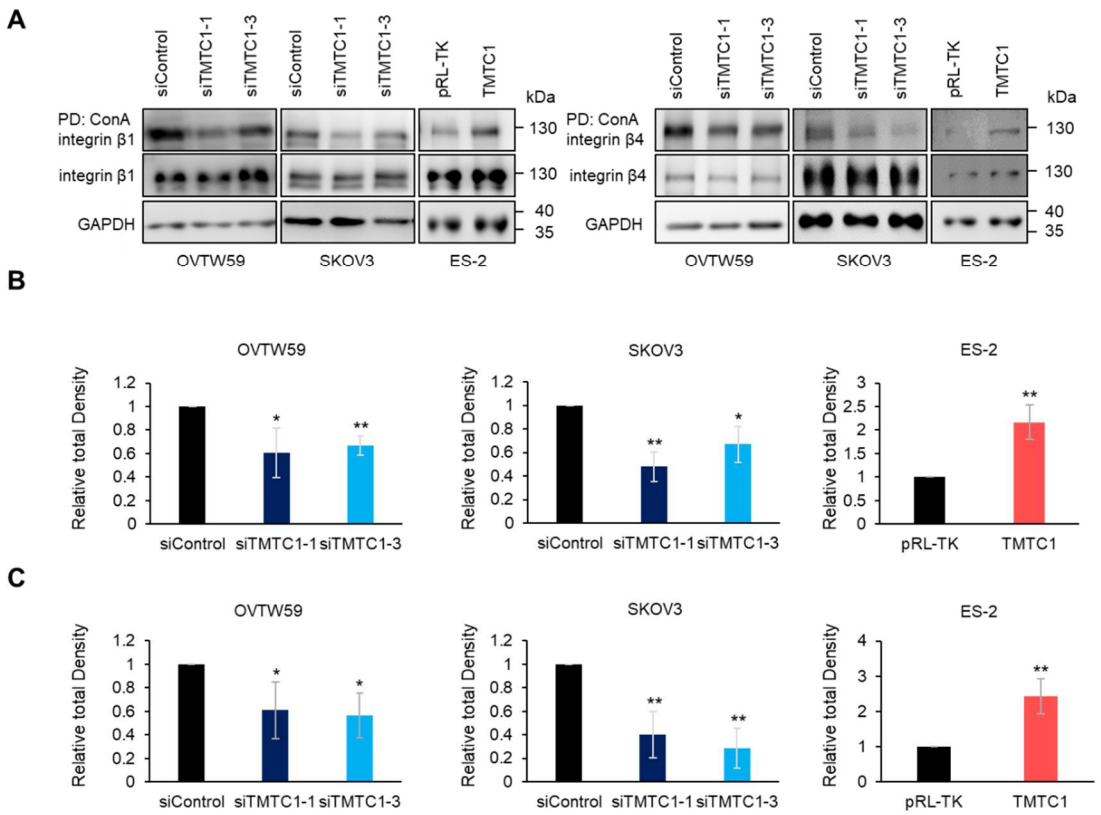

Figure 12. TMTC1 modifies the O-Man glycosylation of integrin β1 and integrin β4 in ovarian cancer cells. (A) ConA pull-down assay was performed to investigate the O-Man glycosylation of integrin β1 and β4. *TMTC1* siRNAs were used to knock down *TMTC1* in OVTW59 and SKOV3 cells. Transfecting TMTC1/pRL-TK plasmid or empty pRL-TK plasmid into ES-2 cells allows for TMTC1 overexpression. Total lysates were subjected to treatment with PNGase F and then pulled down using ConA-agarose beads. GAPDH was utilized as the internal control for loading in these experiments. (B) The integrin β1 levels were quantified from Western blots depicted in Figure 12A of ovarian cancer cells. The relative signal intensities of integrin β1 were quantified using the Visionworks software. (C) The integrin β4 levels were quantified

doi:10.6342/NTU202302473

from Western blots depicted in Figure 12A of ovarian cancer cells. The relative signal intensities of integrin β4 were quantified using the Visionworks software. The data were expressed as the mean ± SD. *P < 0.05; **P < 0.01.

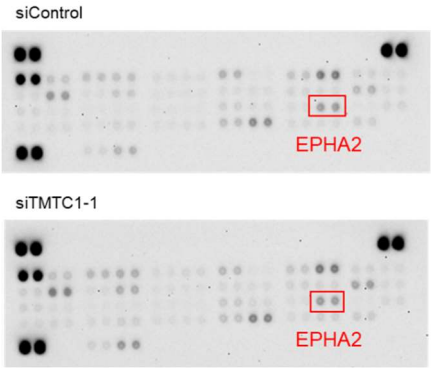

Figure 13. Effects of TMTC1 on phospho-RTK levels. *TMTC1* knockdown did not significantly affect the levels of phospho-RTKs, such as p-EPHA2 (highlighted in red rectangles). OVTW59 cells were subjected to transfection with siRNAs, including siControl or siTMTC1-1. After a 24-hour serum starvation period, the cells were subjected to a 15-minute treatment with 10% FBS. The analysis of phospho-RTKs was conducted using a human phospho-RTK array from R&D Systems, following the manufacturer's protocol, and detected by Western blotting.

doi:10.6342/NTU202302473

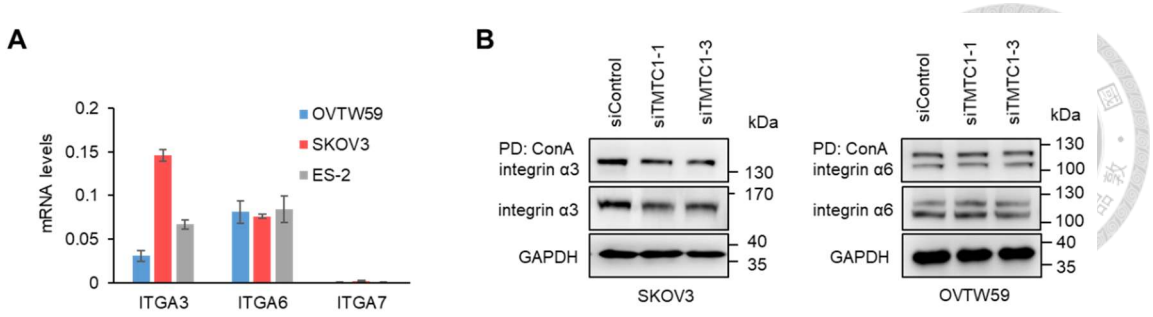

Figure 14. Integrins, α3, α6 and α7 levels and ConA pull-down assays in ovarian cancer cells. (A) The real-time RT-PCR analysis was employed to determine the *ITGA3*, *ITGA6*, and *ITGA7* mRNA levels in ovarian cancer cells. The transcript levels of TMTC1 were analyzed using real-time RT-PCR and normalized to the mRNA levels of GAPDH, resulting in the formation of relative transcript levels. The data was reported as the mean ± SD. n = 3. (B) ConA pull-down assay was performed to investigate the integrin α3 and α6 O-Man glycosylation. SKOV3 and OVTW59 cells were transfected with siControl or two different *TMTC1* siRNA. Cell lysates were subjected to treatment with PNGase F and followed by pull-down using ConA-agarose beads. Signal intensity changes in Integrin α3 and α6 were assessed using Western blotting, with GAPDH serving as the internal control.

doi:10.6342/NTU202302473

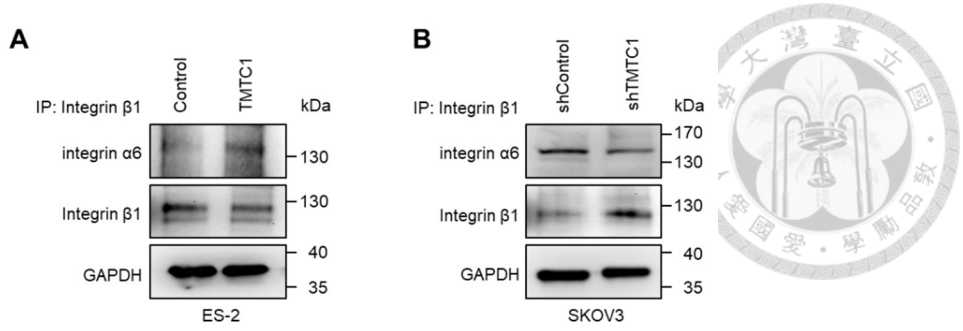

Figure 15. TMTC1 slightly increases the heterodimerization of integrin α6 and integrin β1. (A) The co-IP was performed to investigate the interaction between integrin β1 and integrin α6 in ES-2 cells. Cell lysates derived from both TMTC1-overexpressing and control ES-2 cells were subjected to immunoprecipitation (IP) using an anti-integrin β1 antibody and then immunoblotted with an anti-integrin α6 or anti-integrin β1 antibody. GAPDH was used as a loading control. (B) Co- IP assay was performed to investigate the interaction between integrin β1 and integrin α6 in SKOV3 cells.

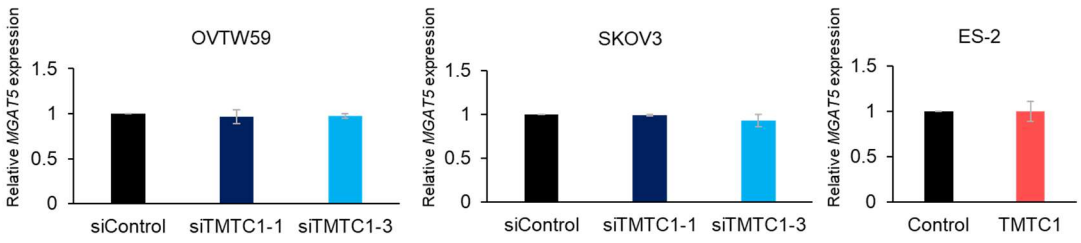

Figure 16. TMTC1 had no effect on the mRNA expression of *MGAT5*. The expression levels of *MGAT5* mRNA were examined by performing real-time RT-PCR analysis in OVTW59 and SKOV3 cells where TMTC1 was knocked down, as well as in ES-2 cells that overexpressed TMTC1. The transcript levels of *MGAT5* were

doi:10.6342/NTU202302473

normalized to the mRNA levels of GAPDH, resulting in the formation of relative transcript levels.

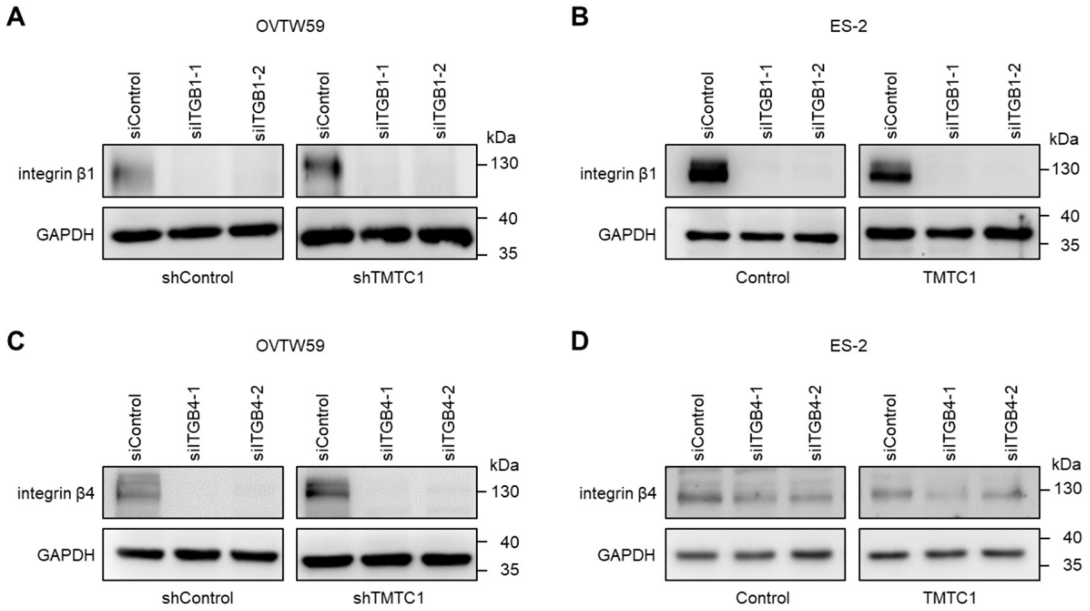

Figure 17. Knockdown of *ITGB1* or *ITGB4* in ovarian cancer cells. (A) Western blots were performed to demonstrate the knockdown of *ITGB1* in OVTW59 cells that were stably transducted with either control shRNA (shControl) or TMTC1 knockdown shRNA (shTMTC1). *ITGB1* was subjected to knockdown using two distinct siRNAs (siITGB1-1 and siITGB1-2). A non-targeting siRNA (siControl) was utilized as a control in these experiments. (B) Western blots showed ITGB1 knockdown in ES-2 cells that were stably transducted with either pLAS2w.Ppuro (Control) or pLAS2w.Ppuro-TMTC1-HA (TMTC1) overexpression vector. (C) Western blots were performed to demonstrate the knockdown of *ITGB4* in OVTW59 cells that were stably

doi:10.6342/NTU202302473

transducted with either control shRNA (shControl) or TMTC1 knockdown shRNA (shTMTC1). *ITGB4* was knocked down using two independent siRNAs (siITGB4-1 and siITGB4-2). A non-targeting siRNA (siControl) was utilized as a control in these experiments. (D) Western blots showing knockdown of *ITGB4* in ES-2 cells that were stably transducted with either Control or TMTC1 overexpression vector.

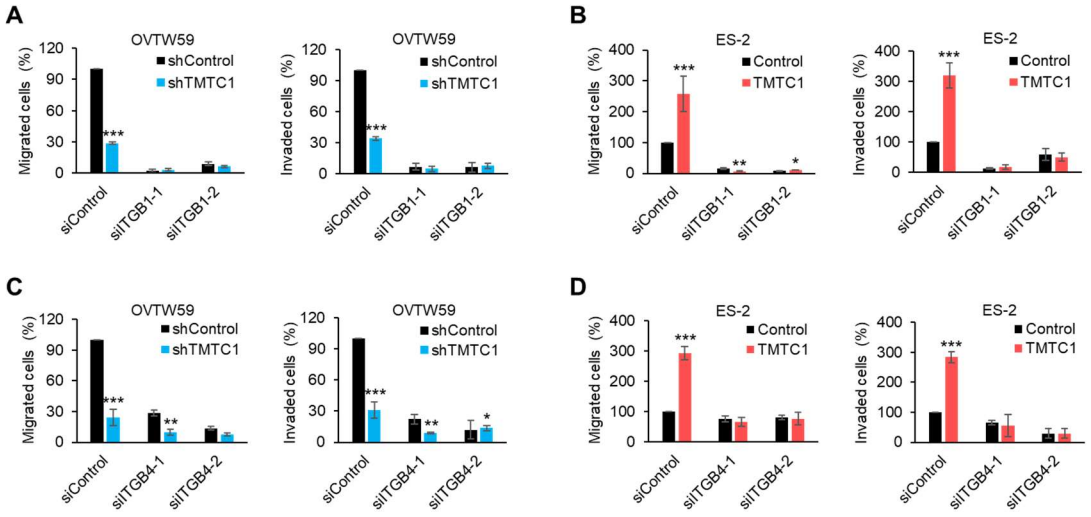

Figure 18. ITGB1 or ITGB4 knockdown can reverse the TMTC1-induced effects on malignant phenotypes. (A) The inhibitory effects of ITGB1 siRNAs on transwell migration and Matrigel invasion were observed in OVTW59 cells with TMTC1 knockdown. OVTW59 cells stably transducted with the shControl or shTMTC1 were transiently transfected with siITGB1-1 or siITGB1-2. The migration and invasion capabilities of these cells were assessed using the Transwell migration assay and Matrigel invasion assay, respectively. (B) The enhanced migration and invasion

doi:10.6342/NTU202302473

induced by TMTC1 in ES-2 cells were reversed upon treatment with ITGB1 siRNAs. The ES-2 cells were stably transducted with Control or TMTC1 overexpression vector and were transiently transfected with siITGB1-1 or siITGB1-2. (C) The inhibitory effects of ITGB4 siRNAs on cell migration and invasion were observed to block the effects of TMTC1 knockdown in OVTW59 cells. The OVTW59 cells stably transducted with the shControl or shTMTC1 shRNA were transiently transfected with siITGB4-1 or siITGB4-2. (D) The increased migration and invasion observed in ES-2 cells due to TMTC1 overexpression were reversed when ITGB4 siRNAs were used. The ES-2 cells were stably transducted ES-2 cells with Control or TMTC1 overexpression vector and were transiently transfected with siITGB4-1 or siITGB4-2. *P < 0.05; **P < 0.01; ***P < 0.001. Results are presented as mean ± SD (n = 3). Data were analyzed using the Student's t-test.

doi:10.6342/NTU202302473

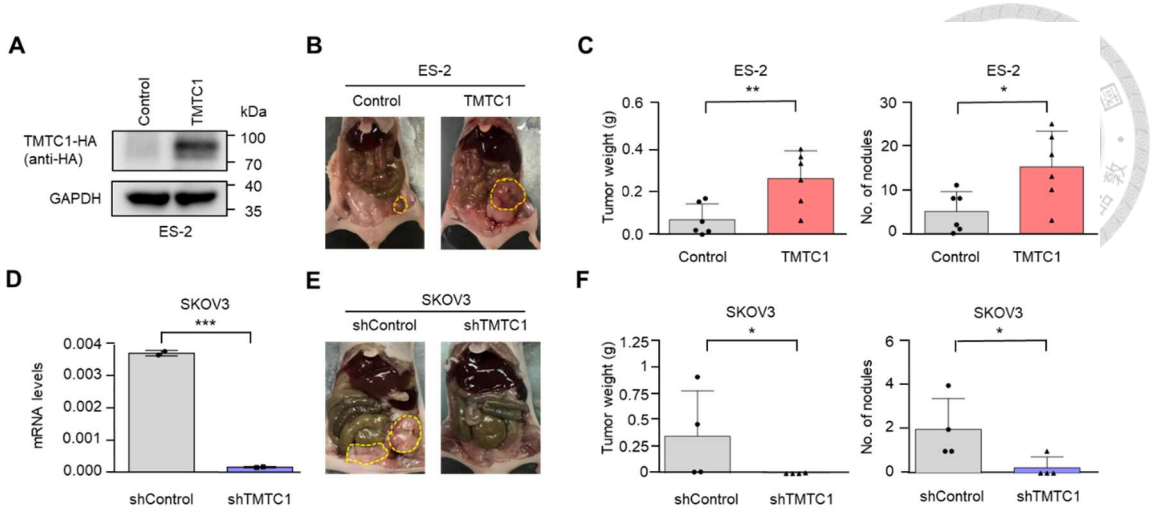

Figure 19. TMTC1 effect on growth and metastasis of peritoneal tumors *in vivo.*

(A) TMTC1-overexpressed ES-2 cells were generated. The HA-tagged TMTC1 protein was subsequently isolated using HA-tag agarose beads and analyzed by immunoblotting using an anti-HA antibody. (B) The representative images display tumor formation (highlighted by yellow circles) in nude mice that received intraperitoneal injections of either control ES-2 cells or TMTC1-overexpressed ES-2 cells. (C) Statistical analyses were conducted to evaluate the tumor weights and nodule numbers obtained from mice after 15 days of cell injection. Each group consisted of six samples in total. *P < 0.05; **P < 0.01. The data were subjected to analysis using the Student's t-test. (D) Under the condition of *TMTC1* knockdown in SKOV3 cells. TMTC1 relative transcript levels of stable transfectants of SKOV3 cells were quantified using real-time RT-PCR. The obtained results were normalized to the mRNA levels of GAPDH, resulting in the formation of relative transcript levels. Representative results

doi:10.6342/NTU202302473

from three independent experiments were shown. (E) Representative images displaying tumor formation, indicated by yellow circles, in nude mice that received intraperitoneal injections of TMTC1 knockdown cells or control SKOV3 cells. (F) Statistical analyses were conducted to evaluate the tumor weights and nodule numbers obtained from mice after 40 days of cell injection. Each group consisted of four samples in total. The data were subjected to analysis using either the Mann-Whitney U test or a one-tailed Student's t-test. *P < 0.05.

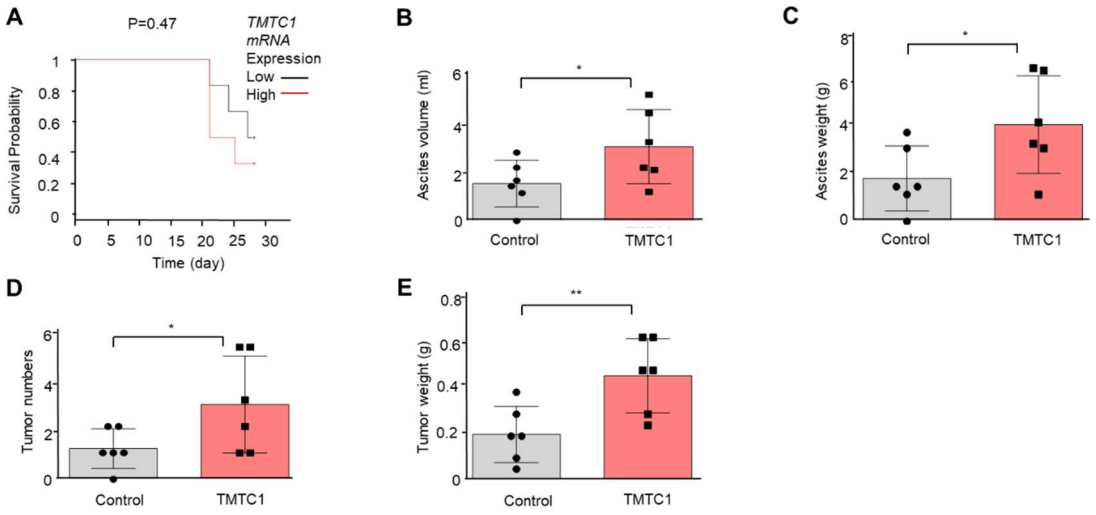

Figure 20. Effects of TMTC1 on survival. (A) Statistical analyses of Survival. P = 0.47 (B)(C) Statistical analyses of ascites volume and weight. *P < 0.05. Data were analyzed using the one-tailed Student's t-test. (D)(E) The statistical analysis of tumor weights and nodule numbers was presented in the figures. The data were subjected to

doi:10.6342/NTU202302473

analysis using a one-tailed Student's t-test. *P < 0.05. **P < 0.01. Each group consisted of six samples in total.

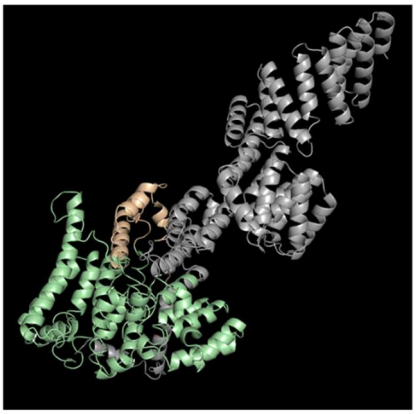

Figure 21. TMTC1 docking results. The protein structure of TMTC1. Molecular docking analysis of TMTC1 was shown.

doi:10.6342/NTU202302473

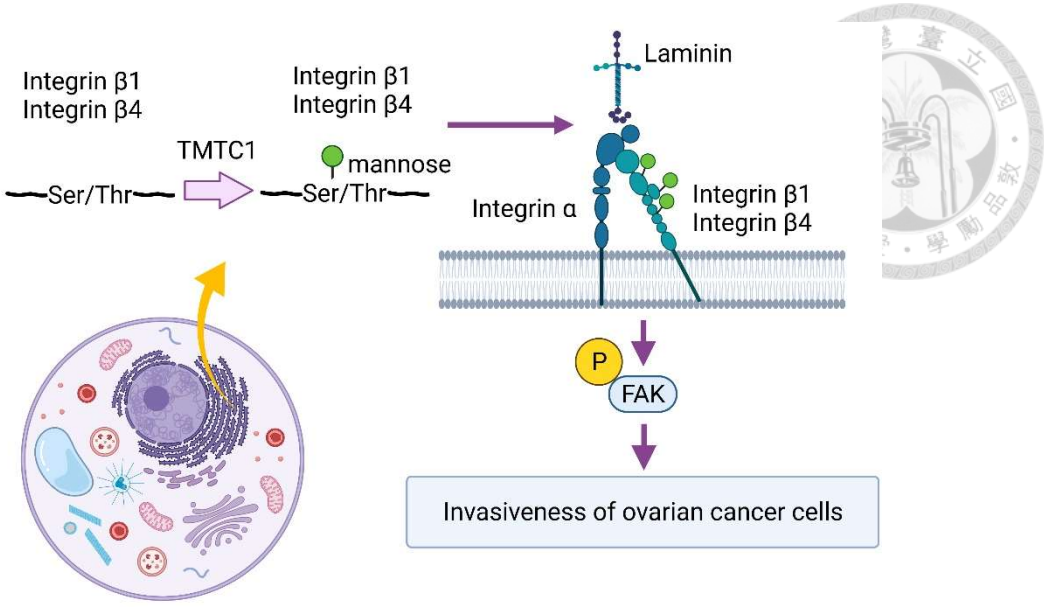

Figure 22. The mechanism proposed for the enhancement of invasiveness in ovarian cancer cells by TMTC1. TMTC1 modifies the O-Man glycosylation of integrins β1 and β4, leading to increased binding to laminin and phosphorylation of FAK, ultimately promoting the invasiveness of ovarian cancer cells. This figure was created using BioRender software.

doi:10.6342/NTU202302473

Tables

Table 1. Univariate and multivariate analysis of prognostic factors for overall survival of ovarian cancer patients (n=116) [a]

Variables	No.[b]	Univariate		Multivariate	
		HR (95% CI) [c]	*p*-value	HR (95% CI) [c]	*p*-value
Age					
≤50	52	1	0.615	1	0.668
>50	64	1.14 (0.69–1.90)		0.89 (0.52–1.52)	
Lymph node					
Negative	87	1	**< 0.001**	1	**0.003**
Positive	29	5.42 (3.23–9.10)		2.98 (1.45–6.13)	
Distant metastasis					
No	96	1	**< 0.001**	1	**0.002**
Yes	20	6.62 (3.72–11.79)		3.46 (1.57–7.60)	
Histologic type					
Serous	71	1		1	
Non-serous	45	0.58 (0.33–0.99)	**0.046**	1.06 (0.58–1.91)	0.861
TMTC1					
Low	43	1	**0.050**	1	**0.030**
High	73	1.72 (1.00–2.95)		1.89 (1.06–3.35)	

[a]Fourteen cases were excluded from the tissue microarray data (Biomax HOvaC154Su01) due to specimens from metastatic sites. Additionally, 8 cases were excluded due to rare histologic types, and 8 cases were excluded due to missing data. The final dataset included 2 clear cell types, 13 endometrioid, 57 high-grade serous, 14 low-grade serous and 30 mucinous. [b] Number of patients

[c] HR, hazard ratio (CI, confidence interval) of univariate or multivariate Cox regression analysis

doi:10.6342/NTU202302473

Table 2. The candidate protein substrates of TMTC1 were identified by LC-MS/MS analysis in OVTW59 cells analysis in OVTW59 ovarian cancer cells.

Gene names	Control (Normalized abundances)	TMTC1 KD [a] (Normalized abundances)	Subcellular location	Ratio (TMTC1/ Control)
PRXL2A	761946.9	0	Secreted	0
EPHA2	308396.5	0	plasma membrane	0
ITGB1	305463.1	0	plasma membrane	0
ATP2B1	3158574.0	0	plasma membrane	0
ITGB4	11560705.0	621522.5	plasma membrane	0.053762
DSG1	1761521.0	198764.4	plasma membrane	0.112837
S100A9	1551257.0	198481.3	Secreted	0.127949
FABP5	3143134.0	437938.6	Secreted	0.139332
PDCD6IP	1328523.0	204573.8	Secreted	0.153986
IDE	914204.0	201437.4	Secreted	0.220342
DCD	3794587.0	933768.9	Secreted	0.246079
ANXA2	8351029.0	2352683.0	Secreted	0.281724
MYOF	32236635.0	10363300.0	plasma membrane	0.321476
LGALS7	1263902.0	416478.5	Secreted	0.329518
CLIC1	2559495.0	982493.0	plasma membrane	0.383862
ARL6IP5	692811.9	268395.8	plasma membrane	0.387401
NCEH1	1095194.0	477185.5	plasma membrane	0.435709

[a]KD, knockdown

doi:10.6342/NTU202302473

Table 3. Table 3. Protocadherin-7 was identified through LC-MS/MS analysis in OVTW59 cells.

Gene names	Control (Normalized abundances)	TMTC1 KD [a] (Normalized abundances)	Ratio (TMTC1 KD/ Control)
PCDH7	19395773.21	16928202.03	0.872778

[a]KD, knockdown

doi:10.6342/NTU202302473

Table 4. The top 10 pathways associated with potential TMTC1 protein substrates were analyzed using the BioPlanet database.

Index	Name	*P*-value	Adjusted *p*-value	Odds Ratio	Combined score
1	Integrin family cell surface interactions	0.0002184	0.02337	110.88	934.67
2	Support of platelet aggregation by Eph kinases and ephrins	0.006781	0.05244	178.36	890.65
3	CHL1 interactions	0.006781	0.05244	178.36	890.65
4	Alpha-4 beta-7 integrin signaling	0.007625	0.05244	156.05	760.96
5	Type I hemidesmosome assembly	0.007625	0.05244	156.05	760.96
6	Reduction of cytosolic calcium levels	0.008469	0.05244	138.71	661.82
7	Monocyte and it's surface molecules	0.009313	0.05244	124.83	583.76
8	Apoptotic cleavage of cell adhesion proteins	0.009313	0.05244	124.83	583.76
9	Integrin beta-4 pathway	0.009313	0.05244	124.83	583.76
10	Platelet adhesion to exposed collagen	0.01100	0.05563	104.02	469.12

doi:10.6342/NTU202302473

Table 5. The Top 10 potential TMTC1 protein substrates identified by LC-MS/MS analysis in SKOV3 ovarian cancer cells.

Gene names	Control (Normalized abundances)	TMTC1 KD [a] (Normalized abundances)	Subcellular location	Ratio (TMTC1 KD/ Control)
CAPN2	8717518	0	plasma membrane	0
PDIA3	3385327	0	Secreted	0
NT5E	1897834	0	plasma membrane	0
CTSD	5196157	0	Secreted	0
LAMP1	21490931	4977159.48	plasma membrane	0.231593
SERPINB2	32157216	12482536.6	Secreted	0.388172
TRPV4	28317374	12853049.3	plasma membrane	0.453893
CALR	43407782	23189430.7	Secreted	0.534223
M6PR	6889177	3734343.9	Secreted	0.54206
ITGB1	14269552	9150575.57	plasma membrane	0.641266

[a]KD, knockdown

doi:10.6342/NTU202302473

Table 6. The top 10 therapeutic potential compounds of targeting TMTC1 were listed.

Accession Number	Vina Result	Name
DB02626	-21.7	Phenylferricrocin-iron
DB14792	-19.9	AZD-5991*
DB12983	-19.7	Phthalocyanine*
DB12352	-18.8	Bizelesin*
DB14555	-18.7	Ursadiol*
DB12651	-18.5	Bardoxolone*
DB12513	-18.4	Omaveloxolone*
DB00602	-18.3	Ivermectin
DB00416	-18.2	Metocurine iodide
DB01199	-18.0	Tubocurarine

doi:10.6342/NTU202302473

Appendix

DNA Sequence of pRL-TK-hTMTC1

agatctaaatgagtcttcggacctcgcgggggccgcttaagcggtggttagggtttgtctgacgcgggggggaggggggaaggaacg
aaacactctcattcggaggcggctcggggtttggtcttggtggccacgggcacgcagaagagcgccgcgatcctcttaagcacccc
cccgccctccgtggaggcgggggtttggtcggcgggtggtaactggcgggccgctgactcgggcgggtcgcgcgccccagagt
gtgacctttteggtctgctcgcagacccccgggcggcgccgccgcggcggcgacgggctcgctgggtcctaggctccatgggga
ccgtatacgtggacaggctctggagcatccgcacgactgcggtgatattaccggagaccttctgcgggacgagccgggtcacgcg
gctgacgcggagcgtccgttgggcgacaaacaccaggacggggcacaggtacactatcttgtcacccggaggcgcgagggactg
caggagcttcagggagtggcgcagctgcttcatccccgtggcccgttgctcgcgtttgctggcggtgtccccggaagaaatatatttg
catgtctttagttctatgatgacacaaaccccgcccagcgtcttgtcattggcgaattcgaacacgcagatgcagtcggggcggcgcg
gtcccaggtccacttcgcatattaaggtgacgcgtgtggcctcgaacaccgagcgaccctgcagcgacccgcttaaaagcttgattct
tctgacacaacagtctcgaacttaagctgcagaagttggtcgtgaggcactgggcaggtaagtatcaaggttacaagacaggtttaag
gagaccaatagaaactgggcttgtcgagacagagaagactcttgcgtttctgataggcacctattggtcttactgacatccactttgcct
ttctctccacaggtgtccactcccagttcaattacagctcttaaggctagagtacttaatacgactcactataggctagcATGAACC
CATTCTACTTTCATGCAGTAAATATAATTTTACACTGCTTAGTGACTCTTGTGCTGA
TGTACACCTGTGATAAAACTGTCTTCAAGAATCGTGGACTTGCTTTTGTAACGGC
ATTGCTTTTTGCTGTACATCCTATTCATACTGAGGCGGTGGCTGGGATCGTTGGCA
GAGCGGACGTGTTAGCGTGTCTGCTGTTTCTATTGGCCTTTCTCTCGTACAACAG
GAGTCTGGATCAGGGCTGTGTTGGGGGAAGTTTCCCTTCCACGGTGTCcCCCTTC
TTCTTGCTGCTCAGTTTGTTTCTGGGGACCTGTGCGATGCTGGTGAAAGAGACAG
GCATCACGGTGTTTGGAGTGTGCTTGGTTTATGACCTCTTTTCCCTTTCCAACAAG
CAAGACAAGTCGAGCAATGGGGCCCTCTGTCCACGCAGCCCACAGCAGCCCGG
GAGCCCCCAGCCCTCCTCACTGCCAGGCCATCCTCACCGGGAGAATGGGAAGCA
GCAGCGGTTCCCTCACAAAGGAGCTTGGGGTGGCTGCCACTCTCCACTGCCACC
AGAACCCAAGAGCAGTGGATTCCCAGTGTCCCCACGAGCTGTGTGGTCCATGAT
GAGATTCCTCACCTATTCCTACCTCTTGGCCTTCAATGTGTGGCTTCTGCTTGCAC
CCGTGACCCTGTGCTATGACTGGCAGGTCGGCAGTATTCCTCTGGTAGAGACCAT
ATGGGACATGCGGAACTTAGCCACCATCTTTCTGGCGGTTGTGATGGCCTTATTGA
GCCTGCACTGCTTAGCAGCCTTTAAGAGACTGGAGCACAAGGAGGTTTTAGTCG
GCTTGTTGTTCCTGGTGTTCCCGTTCATTCCAGCCAGCAACCTCTTCTTCAGGGTG
GGTTTTGTGGTGGCGGAGAGAGTCCTTTACATGCCTAGCATGGGCTACTGCATCC
TTTTTGTGCAcGGACTGAGCAAGCTCTGCACTTGGCTGAATCGATGTGGGGCCAC
CACCCTGATTGTGTCCACTGTGTTGCTGCTGTTGCTTTTCTCTTGGAAAACTGTGA
AACAGAATGAAATTTGGCTGTCAAGAGAGTCCCTATTCAGGTCTGGAGTTCAAAC
TCTGCCCCACAATGCCAAGGTTCACTACAACTATGCCAATTTCCTGAAGGACCAA
GGTCGGAACAAGGAAGCGATCTACCACTACAGAACAGCTCTCAAGTTGTATCCA
CGCCATGCAAGTGCGCTCAACAACCTTGGAACACTGACGAGAGACACAGCAGA
GGCAAAGATGTACTATCAGAGGGCTCTCCAGCTCCATCCACAGCATAACCGGGCT
CTTTTCAATCTGGGGAATCTCCTCAAGTCCCAGGAGAAAAAGGAAGAAGCTATC
ACCTTACTGAAGGATTCCATCAAATATGGTCCAGAGTTTGCAGATGCATATTCAAG

doi:10.6342/NTU202302473

TCATTTCTGAACTTTTTTTCACAAAAGGAAACCAATTAAGAGAGCAGAACCTTCT
CGACAAAGCTTTTGAGAGCTATAGAGTGGCTGTGCAACTAAACCCAGACCAAGC
ACAGGCCTGGATGAACATGGGTGGCATCCAACACATCAAGGGAAAATATGTGTCT
GCAAGAGCTTATTATGAGAGAGCCTTACAGCTGGTTCCAGACAGCAAACTGCTG
AAGGAAAATCTTGCCAAATTGGATCGCCTAGAAAAACGATTACAAGAAGTTCGA
GAAAAGGATCAAACATAGtctagagcggccgcttcgagcagacatgataagatacattgatgagtttggacaaacc
acaactagaatgcagtgaaaaaaatgctttatttgtgaaatttgtgatgctattgctttatttgtaaccattataagctgcaataaacaagtta
acaacaacaattgcattcattttatgtttcaggttcagggggaggtgtgggaggttttttaaagcaagtaaaacctctacaaatgtggtaa
aatcgataaggatccaggtggcacttttcggggaaatgtgcgcggaacccctatttgtttatttttctaaatacattcaaatatgtatccgct
catgagacaataaccctgataaatgcttcaataatattgaaaaaggaagagtatgagtattcaacatttccgtgtcgcccttattccctttttt
tgcggcattttgccttcctgtttttgctcacccagaaacgctggtgaaagtaaaagatgctgaagatcagttgggtgcacgagtgggtta
catcgaactggatctcaacagcggtaagatccttgagagttttcgccccgaagaacgttttccaatgatgagcacttttaaagttctgcta
tgtggcgcggtattatcccgtattgacgccgggcaagagcaactcggtcgccgcatacactattctcagaatgacttggttgagtactc
accagtcacagaaaagcatcttacggatggcatgacagtaagagaattatgcagtgctgccataaccatgagtgataacactgcggc
caacttacttctgacaacgatcggaggaccgaaggagctaaccgcttttttgcacaacatgggggatcatgtaactcgccttgatcgtt
gggaaccggagctgaatgaagccataccaaacgacgagcgtgacaccacgatgcctgtagcaatggcaacaacgttgcgcaaact
attaactggcgaactacttactctagcttcccggcaacaattaatagactggatggaggcggataaagttgcaggaccacttctgcgct
cggcccttccggctggctggtttattgctgataaatctggagccggtgagcgtgggtctcgcggtatcattgcagcactggggccaga
tggtaagccctcccgtatcgtagttatctacacgacggggagtcaggcaactatggatgaacgaaatagacagatcgctgagatagg
tgcctcactgattaagcattggtaactgtcagaccaagtttactcatatatactttagattgatttaaaacttcatttttaatttaaaaggatcta
ggtgaagatccttttgataatctcatgaccaaaatcccttaacgtgagttttcgttccactgagcgtcagaccccgtagaaaagatcaaa
ggatcttcttgagatcctttttttctgcgcgtaatctgctgcttgcaaacaaaaaaaccaccgctaccagcggtggtttgtttgccggatca
agagctaccaactctttttccgaaggtaactggcttcagcagagcgcagataccaaatactgttcttctagtgtagccgtagttaggcca
ccacttcaagaactctgtagcaccgcctacatacctcgctctgctaatcctgttaccagtggctgctgccagtggcgataagtcgtgtct
taccgggttggactcaagacgatagttaccggataaggcgcagcggtcgggctgaacgggggttcgtgcacacagcccagcttg
gagcgaacgacctacaccgaactgagatacctacagcgtgagctatgagaaagcgccacgcttcccgaagggagaaaggcggac
aggtatccggtaagcggcagggtcggaacaggagagcgcacgagggagcttccagggggaaacgcctggtatctttatagtcctg
tcgggtttcgccacctctgacttgagcgtcgatttttgtgatgctcgtcaggggggcggagcctatggaaaaacgccagcaacgcgg
ccttttacggttcctggccttttgctggccttttgctcacatggctcgac

doi:10.6342/NTU202302473